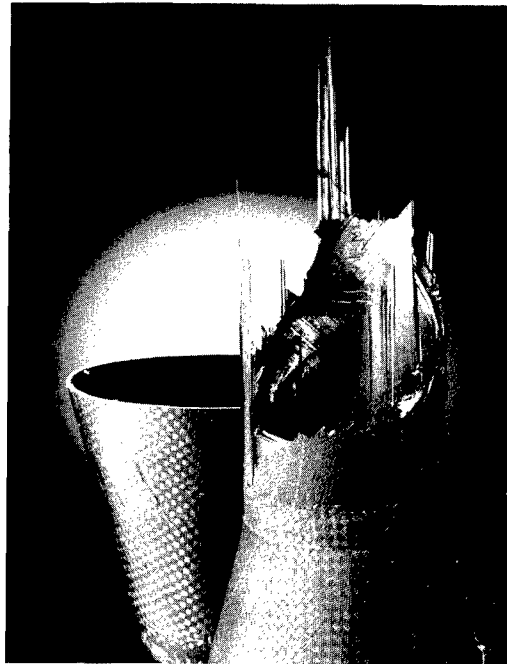


AFOSR TR 97-0712

REPORT DOCUMENTATION PAGE			Form Approved OMB No. 0704-0188	
Public reporting burden for this collection of information is estimated to average 1 hour per response, including the time for reviewing instructions, searching existing data sources, gathering and maintaining the data needed, and completing and reviewing the collection of information. Send comments regarding this burden estimate or any other aspect of this collection of information, including suggestions for reducing this burden, to Washington Headquarters Services, Directorate for Information Operations and Reports, 1215 Jefferson Davis Highway, Suite 1204, Arlington, VA 22202-4302, and to the Office of Management and Budget, Paperwork Reduction Project (0704-0188), Washington, DC 20503.				
1. AGENCY USE ONLY (Leave blank)		2. REPORT DATE November 14, 1997	3. REPORT TYPE AND DATES COVERED Final Technical Report 15 Aug 92 to 14 Aug 97	
4. TITLE AND SUBTITLE Structural Response of Oxidation Resistant Carbon-Carbon Composites Under Cyclic and Monotonic Loading			5. FUNDING NUMBERS F49620-92-J-0436	
6. AUTHOR(S) Ozden O. Ochoa				
7. PERFORMING ORGANIZATION NAME(S) AND ADDRESS(ES) Texas Engineering Experiment Station Texas A&M University Department of Mechanical Engineering 332 Wisenbaker Engr Research Center College Station, TX 77843-3000			8. PERFORMING ORGANIZATION REPORT NUMBER	
9. SPONSORING/MONITORING AGENCY NAME(S) AND ADDRESS(ES) AFOSR/NA 110 Duncan Avenue, Rm B115 Bolling AFB, DC 20332-8050			10. SPONSORING/MONITORING AGENCY REPORT NUMBER F49620-92-J-0436	
11. SUPPLEMENTARY NOTES				
12a. DISTRIBUTION AVAILABILITY STATEMENT Approved for public release; distribution unlimited.			12b. DISTRIBUTION CODE	
13. ABSTRACT (Maximum 200 words) Oxidation damage of carbon-carbon laminates at 900°C and its affect on shear modulus, mass loss, and electrical resistance is studied. Preferential fiber bundle oxidation with some matrix cracking is initially observed. Fiber bundles are severely damaged and increased matrix damage is observed with time. Mass loss results indicate oxidation is diffision controlled at 900°C. Shear modulus decreases with increased oxidation time. Electrical resistance increases with increased oxidation time. An increase in the rate of change of the electrical resistance attributed to a change in the oxidation mechanism from preferential fiber bundle damage to matrix indicates that electrical resistance is a matrix-dominated property. A study of the relationships between electrical resistance, shear modulus, and mass loss measurements indicate that electrical resistance measurements may be used as a possible method of damage assessment of oxidation in carbon-carbon.				
14. SUBJECT TERMS			15. NUMBER OF PAGES 46	
			16. PRICE CODE	
17. SECURITY CLASSIFICATION OF REPORT UNCLASSIFIED		18. SECURITY CLASSIFICATION OF THIS PAGE UNCLASSIFIED	19. SECURITY CLASSIFICATION OF ABSTRACT UNCLASSIFIED	20. LIMITATION OF ABSTRACT UL

19971217 031

CENTER FOR MECHANICS OF COMPOSITES



Structural Response of Oxidation Resistant Carbon-Carbon
Composites Under Cyclic and Monotonic Loading

AFOSR Grant No. F46620-92-J-0436

FINAL REPORT

November 14, 1997

Ozden O. Ochoa

Department of Mechanical Engineering

TEXAS ENGINEERING EXPERIMENT STATION

THE TEXAS A&M UNIVERSITY SYSTEM

NOVA ONLINE FULL-TEXT AVAILABLE 8

REPORT DOCUMENTATION PAGE

Form Approved
OMB No. 0704-0188

Public reporting burden for this collection of information is estimated to average 1 hour per response, including the time for reviewing instructions, searching existing data sources, gathering and maintaining the data needed, and completing and reviewing the collection of information. Send comments regarding this burden estimate or any other aspect of this collection of information, including suggestions for reducing this burden, to Washington Headquarters Services, Directorate for Information Operations and Reports, 1215 Jefferson Davis Highway, Suite 1204, Arlington, VA 22202-4302, and to the Office of Management and Budget, Paperwork Reduction Project (0704-0188), Washington, DC 20503.

1. AGENCY USE ONLY (Leave blank)		2. REPORT DATE November 14, 1997	3. REPORT TYPE AND DATES COVERED Final Technical Report 15 Aug 92 to 14 Aug 97	
4. TITLE AND SUBTITLE Structural Response of Oxidation Resistant Carbon-Carbon Composites Under Cyclic and Monotonic Loading			5. FUNDING NUMBERS F49620-92-J-0436	
6. AUTHOR(S) Ozden O. Ochoa				
7. PERFORMING ORGANIZATION NAME(S) AND ADDRESS(ES) Texas Engineering Experiment Station Texas A&M University Department of Mechanical Engineering 332 Wisenbaker Engr Research Center College Station, TX 77843-3000			8. PERFORMING ORGANIZATION REPORT NUMBER	
9. SPONSORING/MONITORING AGENCY NAME(S) AND ADDRESS(ES) AFOSR/NA 110 Duncan Avenue, Rm B115 Bolling AFB, DC 20332-8050			10. SPONSORING/MONITORING AGENCY REPORT NUMBER F49620-92-J-0436	
11. SUPPLEMENTARY NOTES				
12a. DISTRIBUTION AVAILABILITY STATEMENT Approved for public release; distribution unlimited.			12b. DISTRIBUTION CODE	
13. ABSTRACT (Maximum 200 words) Oxidation damage of carbon-carbon laminates at 900°C and its affect on shear modulus, mass loss, and electrical resistance is studied. Preferential fiber bundle oxidation with some matrix cracking is initially observed. Fiber bundles are severely damaged and increased matrix damage is observed with time. Mass loss results indicate oxidation is diffision controlled at 900°C. Shear modulus decreases with increased oxidation time. Electrical resistance increases with increased oxidation time. An increase in the rate of change of the electrical resistance attributed to a change in the oxidation mechanism from preferential fiber bundle damage to matrix indicates that electrical resistance is a matrix-dominated property. A study of the relationships between electrical resistance, shear modulus, and mass loss measurements indicate that electrical resistance measurements may be used as a possible method of damage assessment of oxidation in carbon-carbon.				
14. SUBJECT TERMS			15. NUMBER OF PAGES 46	
			16. PRICE CODE	
17. SECURITY CLASSIFICATION OF REPORT UNCLASSIFIED	18. SECURITY CLASSIFICATION OF THIS PAGE UNCLASSIFIED	19. SECURITY CLASSIFICATION OF ABSTRACT UNCLASSIFIED	20. LIMITATION OF ABSTRACT UL	

Final Report

November 14, 1997

*Structural Response of Oxidation Resistance Carbon-Carbon Composites
Under Cyclic and Monotonic Loading*

AFSR Grant No. F49620-92-J-0436

*Electrical Resistance Measurements
In Carbon-Carbon Laminates*

I. Introduction	4
i. Objective	7
II. Experimental Approach	8
III. Experimental Testing	12
i. Test Matrix	12
ii. Instrumentation	12
iii. Specimen Preparation	15
a. Rheometry Preparation	15
b. Electrical Resistance Preparations	16
iv. Test Procedure	17
IV. Results	19
i. Mass Loss	19
ii. Shear Modulus	19
iii. Electrical Resistance	21
V. Analysis	23
i. Microscopy	24
ii. Diffusion	28
iii. Mass Loss	28
iv. Resistance	28
a. Analytical Time Simulation	28
1. Assumptions	28
2. Bulk Resistance	29
b. Analytical Mass Simulation	33
v. Shear Modulus	38
VI. Conclusions	43
i. Recommendations	44
VII References	45

List of Figures

Figure 1. Carbon-Carbon Sample Specimen _____	7
Figure 2. Electrical Resistance Representation of Carbon-Carbon at 900 °C _____	8
Figure 3. Complex Modulus G^* _____	11
Figure 4. Test Fixture Side View _____	13
Figure 5. Electrical Connections for Two-Point Probe Measurements _____	14
Figure 6. Dynamic Test Spacers _____	16
Figure 7. Rectangular Torsional Fixture _____	16
Figure 8. Pyroduct 597 Coating Locations _____	17
Figure 9. Percent Mass Loss as a Function of Oxidation Time at 900 °C _____	19
Figure 10. Shear Modulus Measurement of a Typical Unoxidized Carbon-Carbon Specimen _____	20
Figure 11. Shear Modulus Degradation Due to Oxidation at 900 °C _____	21
Figure 12. Electrical Resistance versus Oxidation for a Typical C-C Specimen _____	22
Figure 13. Representative Electrical Resistance versus Oxidation Time for Seventeen Individual C-C Specimens _____	22
Figure 14. Cracks in SiC Coating _____	24
Figure 15. Preferential Fiber Bundle Oxidation after Forty Minutes _____	25
Figure 16. Transverse Fiber Bundle Damage _____	25
Figure 17. Initial Matrix Cracking after Twenty Minutes of Oxidation _____	26
Figure 18. Initial Crack Growth after Twenty Minutes _____	27
Figure 19. Matrix Degradation after Sixty Minutes of Oxidation _____	27
Figure 20. Analytical Simulation with Inhibitor Volume Fraction Reduction _____	32
Figure 21. Analytical Simulation with Constant Inhibitor Volume Fraction _____	33
Figure 22. Electrical Resistance versus Percent Mass Loss for Seventeen Specimens _____	37
Figure 23. Representative Electrical Resistance for Seventeen Specimens versus Percent Mass Loss _____	38
Figure 24. Shear Modulus as Compared to Percent Mass Loss at 900°C _____	39
Figure 25. Shear Modulus versus Electrical Resistance for Carbon-Carbon at 900°C _____	40
Figure 26. Experimental Shear Modulus and Analytical Electrical Resistance as Compared to Percent Mass Loss _____	41

List of Tables

Table 1. Test Matrix.	12
Table 2. Analytical Simulation Parameters for Inhibitor Volume Fraction Reduction	32
Table 3. Resistivity Values of C-C Constituents at 900 °C	35
Table 4. Analytical Simulation Parameters for eq(29) and eq(33)	37
Table 5. Shear Modulus and Electrical Resistance Correlation with Mass Loss	41

I. Introduction

Engineering technology has seen advances both in the selection and development of materials. Applications in extreme conditions have required the development of new composite materials. Consequently, composite materials have played an increased role in engineering applications. In particular carbon-carbon composites have become a viable alternative to traditional metals in some aerospace applications. Primary advantages of carbon-carbon are its ability to retain its mechanical properties at extreme temperatures, its toughness, dimensional stability, and specific strength [1,2]. The primary draw back of carbon-carbon is oxidation in an oxygen atmosphere at temperatures in excess of 430°C.

Carbon-carbon consists of carbon fibers embedded in a carbon matrix. Fibers provide support for tensile loading, but they provide little resistance to buckling for compressive loads. Along the fiber direction material properties are strong, but properties transverse to the fiber direction are relatively weak. Attaining better properties in the transverse directions can be achieved using various methods of fiber orientation. Fibers can be chopped, generally between 6 and 13 mm in length, and randomly oriented in the matrix [3]. Groups of fibers, termed fiber bundles or tows, can be woven together in a variety of methods. The easiest weaving technique is to make carbon fiber mats, essentially two dimensional, which can be successively stacked in the carbon matrix. Weaves having fiber bundles oriented at angles other than 0° or 90° are termed angle plies. More complex and costly multidirectional weaving techniques can be also be used to orient fiber bundles giving a three dimensional structure. For example a 4-D weave is a three dimensional structure that has fibers oriented in four directions. Ultimately, the matrix governs the transverse properties of the carbon-carbon composite. The purpose of the carbon matrix is to both hold the fibers together and transfer the loading to the fibers.

Carbon fibers are typically manufactured from rayon, polyacrylonitrile (PAN), or pitches. PAN is a thermoplastic polymer and is currently the most common base for carbon fibers. Converting PAN to carbon fibers begins with the stabilization of the polymer. PAN is a fusible polymer but it must be converted to an infusible configuration so that the fibers do not collapse or lose their chemical orientation during carbonization [1]. PAN fibers are heated to temperatures between 200 °C and 300 °C in an oxygen-containing atmosphere

during the stabilizing process. The fibers are stretched during stabilization to maintain the orientation of the graphene layers in the PAN [1,3]. Subsequently, the carbon content of the fibers is increased by carbonization at temperatures between 1000°C and 1500°C. Carbonization is done in an inert atmosphere primarily to prevent oxidation. Additional stretching can also be implemented to achieve increased crystalline perfection, which yields stronger fibers. Carbonization converts the PAN from a low strength, low modulus polymer with a high strain to failure ($\epsilon_f \approx 10\%$) to a high strength, high modulus ceramic with a low strain to failure ($\epsilon_f \approx 1-2\%$) [1]. Associated density increases and fiber diameter reductions also occur during carbonization. Additional heat treatment above 1800 °C, graphitization, transforms the carbon structure into a graphite structure. Graphitization increases fiber length and fiber strength but reduces the strain to failure of the fiber [1,3]. Carbonization techniques similar to those used in fiber production are also used in the fabrication of the carbon matrix.

Manufacturing of the carbon matrix can be accomplished from either liquid precursors or from gases. Liquid precursors, such as resins, are carbonized under pressure to get the highest carbon yield. Carbonization occurs in an inert atmosphere to prevent oxidation of the fiber and the char. Following carbonization shrinkage occurs, which leads to cracks and the formation of voids. If the fibers used are surface treated the composite will shrink as a whole because of the strong fiber matrix bond. If untreated fibers are used the matrix pulls away from the fibers and will cause voids and little shrinkage will occur in the fiber direction. In order to fill the cracks and voids the carbon-carbon undergoes a densification process by either vacuum or pressure impregnation of additional resin. Subsequently the carbonization process is repeated. There is a mass gain for every impregnation and some mass loss during the carbonization. Overall, carbonization by liquid precursor is a process of diminishing returns.

Carbon char can also be produced using chemical vapor deposition (CVD) or chemical vapor infiltration (CVI). Thermal decomposition of carbonaceous gases, between 800 °C - 1100 °C, onto heated fibers creates the carbon matrix. This technique is usually carried out isothermally at atmospheric pressure. The rate of deposition depends on the temperature, feed gas rate, and the flow rate of the gas. Deposition occurs through diffusion

and no carbon is lost in the process. However, 100% densification is not possible because of pore blockages in the matrix. CVD techniques typically yield highly porous mediums.

Carbon-carbon composite is a porous, brittle medium, a consequence of the manufacturing processes and the carbon itself. The porosity of carbon-carbon can be of both a mechanical benefit and a chemical detriment. Carbon-carbon, though brittle, typically does not fail catastrophically because of its high fracture toughness. Part of this fracture toughness can be attributed to the porosity of the material. Small-scale uniform porosity can be effective both as a crack arrestor and an attenuator of mechanical impulses [1]. Chemically, porosity aids in the process of oxidation of unprotected carbon-carbon at high service temperatures by providing oxygen a means of infiltrating the carbon-carbon substrate. Hence, the density and the associated porosity from manufacturing processes influence the performance of carbon-carbon composite. Oxygen begins to react chemically with carbon-carbon at about 430°C and the result is adsorption of oxygen by the carbon so that gaseous CO and CO₂ are formed [1]. Oxidation of uncoated woven carbon-carbon has shown a reduction in the elastic modulus and flexural strength by 30% and 50% respectively for 10% weight loss. Changes in the flexural failure mode from delamination cracking to predominately cross-bundle cracking, which is related to microstructural changes resulting from oxidation, have also been noted. Oxidation weakens the fiber bundles by selective attack at the fiber/matrix interfaces within the fiber bundles. Bundle/bundle interfaces and interfaces between plies, however, are relatively unaffected [3]. Prevention of oxidation is currently accomplished by the utilization of oxygen inhibitors, as well as external coatings.

No single oxygen inhibitor has been found completely effective over the working temperature range of carbon-carbon, which may include temperatures as high as 1650°C. To resolve this problem a number of inhibitors are used to cover the temperature spectrum. At temperatures between 1000°C and 1800°C ceramic materials are usually chosen to coat the carbon-carbon substrate. The major obstacles to overcome in this temperature range are the interactions, physically, chemically, and mechanically of the inhibitor. Silicon carbide (SiC), one inhibitor that is chemically compatible with carbon-carbon produces a thin layer of silica film which has a low permeability to oxygen. SiC is applied near 1100°C in either an inert atmosphere or vacuum to prevent oxidation of the carbon-carbon substrate being coated. Because of the differences in the coefficients of thermal expansion between SiC and carbon-

carbon, cracks tend to develop in the coating as the SiC cools down below the application temperature [3,4]. This leaves the substrate susceptible to oxidation until the coating can expand and seal itself near 1100°C, the application temperature. Protection below 1000°C is provided by either boron or phosphor based additives. One method of supplying oxidation protection is to impregnate boron carbide (B_4C) into the carbon-carbon substrate. Boron carbide, when heated, chemically reacts with oxygen to form boric oxide (B_2O_3), a stable glass. Near 450°C the viscous glass fills voids and cracks in the substrate and the protective outer SiC coating, thereby inhibiting oxygen penetration and ultimately oxidation. Together these two systems provide a protective barrier, which reduces the rate of oxidation but does not fully prevent it [4]. A sample specimen is represented in Figure 1.

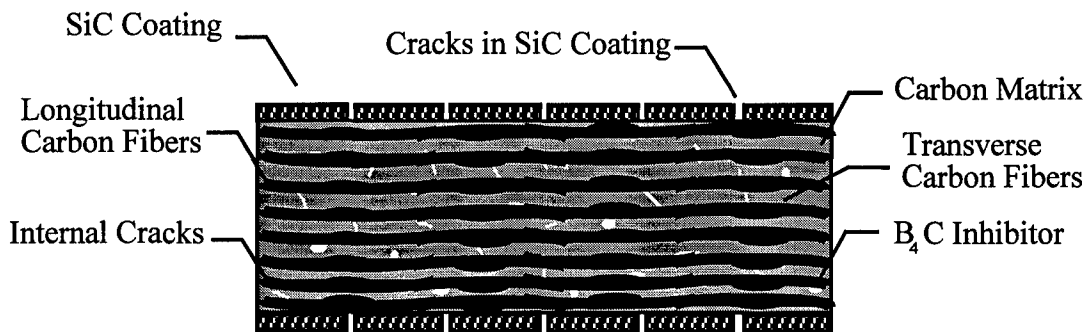


Figure 1. Carbon-Carbon Sample Specimen

i. Objective

Present means of monitoring oxidation of carbon-carbon is primarily done on a mass loss basis [1]. An alternative method, monitoring the changes in electrical resistivity in carbon-carbon, has been proposed as a possible solution to monitor the effects of oxidation. The primary objective of this research is to determine if relationships exist that would allow the use of electrical resistance measurements to determine mass loss and the shear modulus in an oxidized carbon-carbon specimen.

II. Experimental Approach

The carbon-carbon specimens used have four constituents. Silicon carbide (SiC) coating at the top and bottom surfaces of the substrate provides oxidation protection for temperatures above 1093°C. The substrate consists of T-300 carbon fibers, carbon matrix, and the oxidation inhibitor boron carbide (B₄C), which will chemically react with oxygen and become boric oxide (B₂O₃). Each of these four components contributes to the oxidation characterization of the specimen. The simple electrical resistance model for carbon-carbon specimens at 900°C is shown Figure 2 [5].

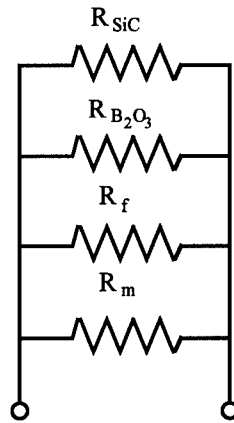


Figure 2. Electrical Resistance Representation of Carbon-Carbon at 900 °C

R_f represents the resistance contribution of the carbon fibers, R_m represents the resistance contribution of the carbon matrix, $R_{B_2O_3}$ represents the total boric oxide contribution, and R_{SiC} represents the total SiC contribution to the bulk resistance of the carbon-carbon substrate. Because the constituents are in parallel the bulk resistance of the carbon-carbon substrate is determined by eq (1).

$$R_{Bulk} = \frac{1}{\frac{1}{R_{SiC}} + \frac{1}{R_m} + \frac{1}{R_f} + \frac{1}{R_{B_2O_3}}} \quad (1)$$

For each individual component resistance is defined as shown in eq (2).

$$R_I = \frac{\rho_I L_I^2}{V_I} \quad (2)$$

where ρ_I is the constituent's resistivity in ohm-m, L is the constituent's length which is equivalent to the specimen's length in meters along the major axis between the potential reading electrical contacts, V_I is the constituent's volume in m^3 and R_I is the resistance in ohms of the respective constituent. Substitution of eq(2) into eq(1) provides the bulk resistance in terms of each constituents respective volume and resistivity.

$$R_{Bulk} = \frac{L^2}{\frac{V_{SiC}}{\rho_{SiC}} + \frac{V_m}{\rho_m} + \frac{V_f}{\rho_f} + \frac{V_{B_2O_3}}{\rho_{B_2O_3}}} \quad (3)$$

It is assumed that the length of the specimen, L , and the respective resistivities, ρ , remain constant for all constituents at $900^\circ C$.

Carbon fibers and the carbon matrix comprise the bulk of the specimen and are the primary conductors. Consequently, changes in bulk electrical resistance will be affected mainly by the degradation of these two constituents. As the carbon fibers and carbon matrix oxidize, their volume in the substrate decreases. Because the volume of the carbon fibers and matrix is inversely proportional to the electrical resistance, an increase in the electrical resistance of the carbon-carbon substrate should occur with increasing oxidation.

Changes in electrical resistance of the carbon-carbon specimen were monitored by the two-point probe method for measuring electrical resistance. Two conditions were taken into account when implementing the two-point probe method. First, measurements were made far enough away from the end on contacts, at least one maximum cross section width of the specimen, to ensure that the potential is being measured across a uniformly distributed current. Secondly, the voltmeter had a high input impedance relative to the impedance of the specimen. Additionally, good electrical contacts were ensured between the oxidized surface and the contacts to eliminate distortion in equipotential lines near the specimen's ends [6]. In order to provide data used in relating the electrical resistance trend to modulus degradation, rheometry was utilized to determine the trends of the in-plane shear modulus. This was accomplished by imposing an oscillatory strain eq(5) on the rectangular specimen

[7]. This strain and the resulting torque eq(6) were measured by a Rheometrics Mechanical Spectrometer/Dynamic Spectrometer RMS-800/RDSII computer to determine the average amplitudes, γ_0 and T_0 , and phase shifts, δ_γ and δ_T , of each, relative to a reference sine wave of fixed amplitude Φ of eq(4). Comparison of the average amplitudes and phase shifts to the reference sine wave determined the lag, δ_γ , between the imposed strain and the reference sine wave. Likewise the phase lag, δ_T , between the resulting torque and the reference sine wave was monitored.

$$\beta = \Phi \sin \omega t \quad \text{Reference sine wave} \quad (4)$$

$$\gamma = \gamma_0 \sin \omega t + \delta_\gamma \quad (5)$$

$$M = T_0 \sin \omega t + \delta_T \quad (6)$$

[8]. The difference between δ_γ and δ_T , was the phase lag, δ , between the imposed strain and the resulting torque. The resulting torque was then expressed as an in-phase and out-of phase component of the resulting torque proportional to δ . The average imposed strain was then converted to percent strain using the following expressions [8].

$$K_\gamma = \frac{T}{L} \left[1 - 0.378 \left(\frac{T}{W} \right)^2 \right] \quad (7)$$

$$\gamma = K_\gamma \theta \quad (8)$$

$$\gamma * 100 = \% \text{ Strain} \quad (9)$$

Where T is the thickness of sample in millimeters, W is the width of sample in millimeters, L is the length of sample in millimeters, K_γ is the strain constant, θ is the actuator angular displacement in radians, and γ is the strain. Similarly the average resulting torque is converted to percent stress as [8].

$$K_\tau = 1000 \left[\frac{3 + 1.8 \left(\frac{T}{W} \right)}{WT^2} \right] G_c \quad (10)$$

$$\tau = K_{\tau} M \quad (11)$$

Where T is the thickness of sample in millimeters, W is the width of sample in millimeters, M is the transducer torque gram-centimeters, K_{τ} is the stress constant, G_c is 98.07 Pascal per gram (SI), and τ is the stress in Pascal. The complex shear modulus of the material, G^* , is defined as

$$G^* = \frac{\tau}{\gamma} \quad (12)$$

Written in complex notation both the real and imaginary component of the modulus are represented as

$$G^* = G' + iG'' \quad (13)$$

G' is the real part of the shear modulus which represents the energy stored elastically in the specimen. G'' is the imaginary part of the shear modulus called the loss modulus; it is an energy dissipation term. The phasor diagram shown in Figure 3 gives the relation of both G' and G'' to G^* [9].

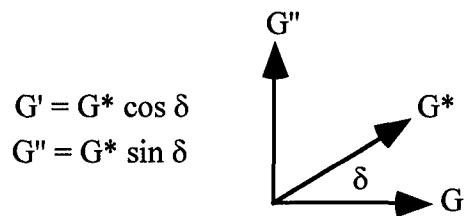


Figure 3. Complex Modulus G^*

The phase lag , δ , in Figure 3 can be expressed as follows [10].

$$\tan \delta = \frac{G''}{G'} \quad (14)$$

Carbon-carbon is a brittle elastic material system, consequently the phase lag δ is small. Therefore, the modulus of the material was approximated by the real part, G' , of the complex modulus G^* .

III. Experimental Testing

i. Test Matrix

Oxidation exposure was accomplished by using two different methods. Three samples #8, #14, #24, and #28 were oxidized at four twenty minute intervals for a cumulative total of eighty minutes of oxidation. Additionally, fifteen specimens were oxidized for a specific time interval of forty minutes, sixty minutes, or eighty minutes. The test matrix is shown in Table 1. An "X" indicates the cumulative exposure times of the respective specimen.

Table 1. Test Matrix.

Oxidation Time in Minutes				
Specimen	20	40	60	80
#8	X	X	X	X
#9		X		
#10				X
#11			X	
#12				X
#13				X
#14	X	X	X	X
#15	X			
#16			X	
#17			X	
#18		X		
#19		X		
#22				X
#23				X
#24	X	X	X	X
#25			X	
#26		X		
#27		X		
#28	X	X	X	X

ii. Instrumentation

Rheometrics Mechanical Spectrometer/Dynamic Spectrometer model RMS-800 RDSII (serial number 0292640) was used for the shear modulus measurements. Rheometrics

Rhios software version 4.4.4 run on an IBM compatible computer was used to control the RMS-800 RDSII, collect the data and store it to an ASCII file for analysis.

The test fixture used for the electrical resistance measurement was fabricated using Rescor 780 alumina oxide castable ceramic. It was chosen for the main body because of its working temperature, 1871°C, its dielectric strength, 200 Volts/Mil, and its mechanical strength, 3000 psi. Three ceramic components form the main body of the test fixture. Two of the components supported the carbon-carbon specimen and housed two horizontal platinum contacts. These pieces were bolted together using three, 1/4" × 20 × 5.25" ceramic threaded rods. The third part was placed over the carbon-carbon specimen and housed two vertical platinum contacts. This component was bolted to the other components using four, 1/4" × 20 × 2" ceramic bolts. Platinum contacts, spaced 22 mm apart, were chosen as the most reliable means of obtaining good electrical contact with the specimen surface. The contacts were made of .032" diameter NiCr wire, 1" × 0.125" × 0.02" rectangular platinum strips, 0.01" diameter platinum wire, Pyroduct 597, and Rescor castable ceramic. The platinum wire was used to bind together the NiCr wire and the platinum strip. Then Aremco products Pyroduct 597 was used to adhere the NiCr wire to both the platinum wire and platinum strip. After curing it was embedded in the Rescor castable ceramic to form the body of the contact. The test fixture is illustrated in Figure 4.

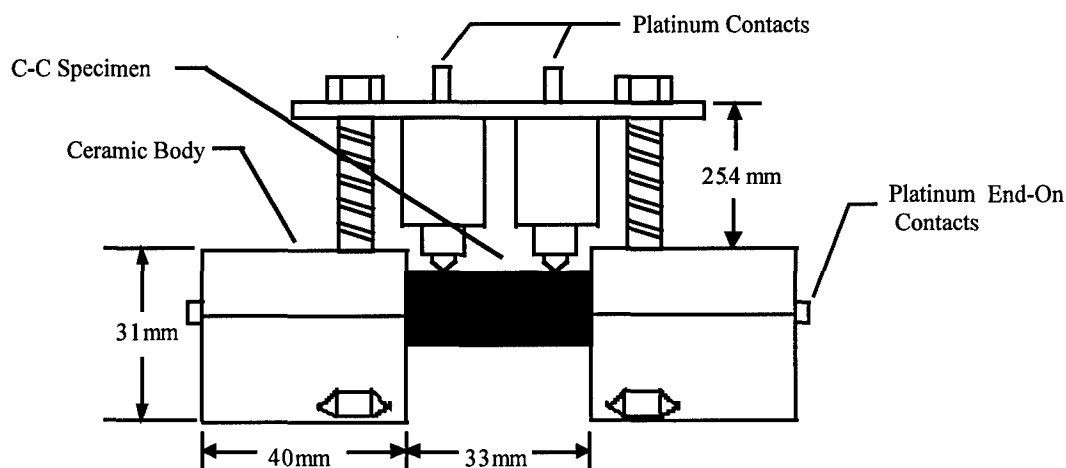


Figure 4. Test Fixture Side View

A Keithley High Voltage Source Measurement Unit (Smu) model 237, serial number 497689, was used to determine the potential readings across the C-C sample. The Keithley Smu was connected to the ceramic specimen holder as shown in Figure 5.

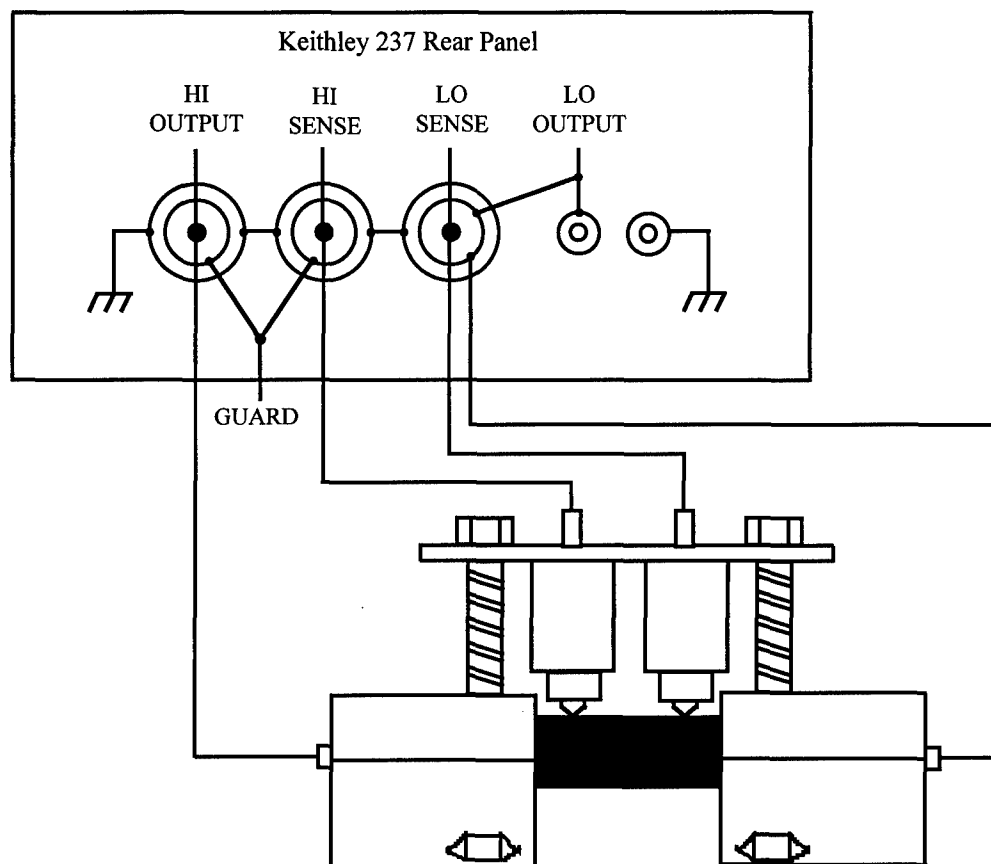


Figure 5. *Electrical Connections for Two-Point Probe Measurements*

A computer program written in Quick Basic in conjunction with an IBM compatible computer was used to control the Keithley Smu and record information through an IEEE-488 connection via Computer Board Incorporated's GPIB board model CIO-PC2A. The program performed the following tasks on the Smu.

- Restored factory defaults on Keithley Smu.
- Set Keithley Smu to source current and measure potential.
- Set Keithley Smu to direct current, D.C., mode.
- Set Keithley filter to average 32 readings as one reading for quieter signal.
- Set Keithley to sense in "remote" as needed for the two-point probe method.
- Set Keithley to "autorange" to automatically sense the potential with the greatest accuracy.

- Set sampling rate to 16.67 msec.

Additionally the program set up the data file to record the data and provided a graphical display for the user.

A Marshall Annealing Furnace model 1079S, serial number 8037-5589, was used to heat the specimen to 900°C. Local specimen temperature was monitored using a type K thermocouple connected to a Fluke 2190A Digital Thermometer, serial number 58912. Temperature was controlled by a type 125 Eurotherm Programmer, serial number 8037-5589. Argon and compressed flow was monitored by a Tylan Flowmeter serial number FF406010.

iii. Specimen Preparation

Specimens of dimensions 3.8mm × 11mm × 46mm were cut from a highly inhibitive carbon-carbon panel material made by HITCO using a diamond blade. The carbon-carbon material has the following characteristics:

- PAN T-300 heat treated fibers (3k filaments yarn).
- 8-harness satin weave, 23X24
- Inhibitors located in carbonized phenolic matrix.
- CVI processing for densification.
- Coating: Surface preparation by laser grooving prior to the RT42 CVD SiC, followed by HITCO's M185 Sealant.

After cutting, the specimens were stored in a desiccant jar. Prior to subjecting the carbon-carbon specimens to testing, the weight, width, and thickness of each sample were measured and recorded.

a. Rheometry Preparation

Rheometrics Mechanical Spectrometer/Dynamic Spectrometer model RMS-800 RDSII (serial number 0292640) in conjunction with Rheometrics Rhios software version 4.4.4 were used for the in shear modulus measurements. Each end of the specimen was inserted into a U-shaped aluminum spacer, see Figure 6, which provided a proper fit when the specimen was placed into the rectangular torsional fixture and prevented the ends of the sample from being damaged.

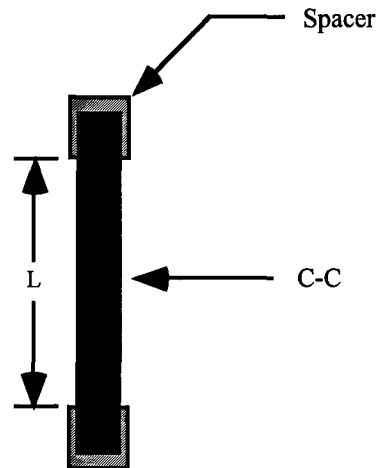


Figure 6. *Dynamic Test Spacers*

Then the sample was mounted into the rectangular torsional fixture using set screws as shown in Figure 7.

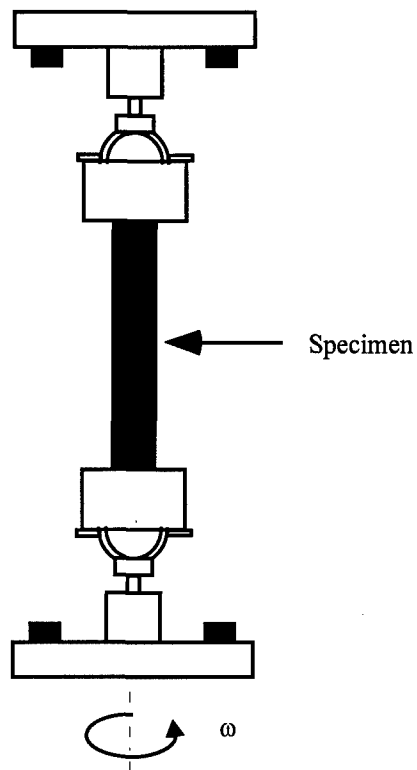


Figure 7. *Rectangular Torsional Fixture*

b. Electrical Resistance Preparations

After shear modulus measurements were taken the specimen was prepared for electrical resistance measurements with Aremco Products' Pyproduct 597. Pyproduct 597 was

place on one side at two locations, approximately 3 mm in width and centered approximately 11 mm from the center of the specimen. Both ends of the C-C specimen were also coated with Pyroduct 597. The coating locations are shown shaded in Figure 8. The coated specimen was then cured at 200 °F for three hours as per instructions.

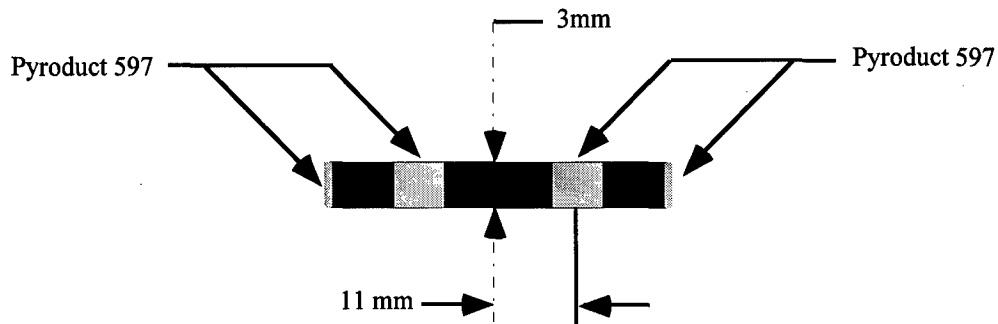


Figure 8. *Pyroduct 597 Coating Locations*

iv. Test Procedure

Preliminary rheometry tests were run at rates of 10, 1, and 0.1 rad/sec to investigate the frequency dependency affects of the shear modulus. Readings at the various rates indicated that the material was relatively frequency independent, hence a strain sweep method was used. The initial strain, final strain, and strain increment used were 0.02%, 0.05%, and 0.005% respectively. These low strains were chosen so as not to damage the specimen or the RMS machine. The following describes the procedure used for the rheometry tests.

Prior to electrical resistance measurements, the shear modulus of the carbon-carbon specimen was determined experimentally using Rheometrics RMS-800 RDSII and Rhios software. Once the specimen was mounted in the aluminum spacers and prior to inserting the specimen into the test fixture, the distance between the inside edges of the spacers was measured at six locations to determine the average length of the specimen. Using the Rhios software the rectangular geometry option was chosen and the specimen's width, length, and thickness were entered into the computer. The strain sweep test option was selected and the initial strain, final strain, and strain increment were then set to 0.02%, 0.05%, and 0.005% respectively. Three tests were then run on each specimen at 10, 1, and 0.1 rad/sec. The results of these tests were then used to get an averaged shear modulus. Subsequently,

electrical resistance readings were taken while the specimen was oxidized using the following procedure.

The Keithley Smu was turned on one hour prior to testing as to ensure the accuracy of the measurements taken. Electrical connections as described in Figure 7 were then made. Using a known resistor, test measurements were taken prior to each test run to ensure proper functioning of both the Keithley Smu and the specimen holder. Following satisfactory test readings the C-C specimen was positioned into the fixture so that the Pyroduct coated regions were contacted by the current carrying contacts on the ends and the potential measuring contacts on the side. Ceramic threaded rods, nuts, and bolts were used to securely fasten the specimen in place as shown in Figure 4. A room temperature resistance reading of the specimen was then taken using the following technique provided by Keithley. A source current of 0 nA was selected and after one potential reading the "suppress" button on the front face of the Smu was pressed. After pressing the "suppress" button the source current was reset to 100 mA. It is reported that measurements taken in this fashion are within 1% [11]. The ceramic specimen holder was then placed inside the quartz tube, which was inside the model 1079S Marshall Annealing Furnace. The endcap was then placed on the end of the tube and the type K thermocouple connected to the Fluke 2190A Digital Thermometer, was inserted into the tube. Its end was position near the specimen holder to measure the specimen's temperature. Using the thumbwheels on the type 125 Eurotherm Programmer the temperature was set to 900°C. As the temperature reached 360°C argon gas was introduced into the quartz tube at a rate of 5 cc/sec to prohibit the specimen from oxidizing between 430°C and 900°C. When the furnace reached 900°C the argon was left on for five minutes to allow the resistance reading to stabilize. Subsequently, compressed air was introduced into the quartz tube at 5 cc/sec for the chosen oxidation period. Once oxidation of the sample was complete, argon was reintroduced into the quartz tube at 5 cc/sec to arrest oxidation in the sample as it cooled to room temperature. Upon completion of the resistance measurements, the specimen was weighed and shear modulus measurement as described above was taken again. Following shear modulus measurement the specimen was then analyzed using SEM.

IV. Results

i. Mass Loss

A linearly increasing trend of the percent mass loss as a function of oxidation time for seventeen individual carbon-carbon specimens each oxidized for twenty, forty, sixty, or eighty minutes is shown in Figure 9. The mass loss is the result of a volume reduction due to fiber loss, matrix loss, and inhibitor volatilization.

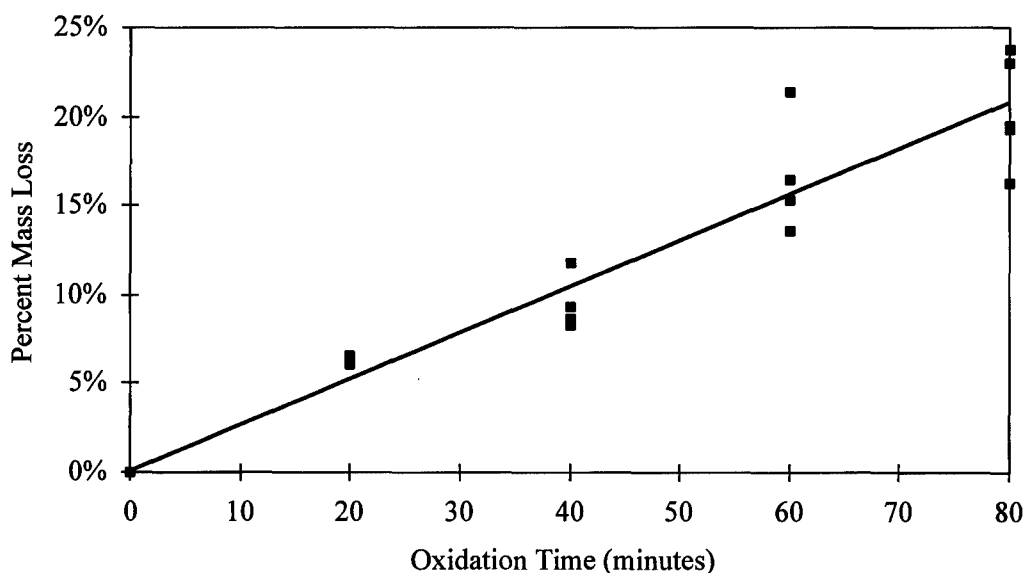


Figure 9. Percent Mass Loss as a Function of Oxidation Time at 900 °C

ii. Shear Modulus

The shear modulus measurements were obtained using Rheometrics RMS-800/RDSII Dynamic Spectrometer prior to oxidation from a typical carbon-carbon specimen at frequencies of 0.1 rad/sec, 1 rad/sec, and 10 rad/sec are shown in Figure 10. The storage modulus, G' , curves show that shear modulus of the carbon-carbon specimen is not frequency dependent; however, a small decrease in G' is observed with an increase in strain. A comparison of the loss modulus, G'' , to G' shows that G'' is much smaller than G' , hence the phase lag, δ , is small, which is characteristic of the highly elastic, brittle carbon-carbon specimen at room temperature. The average shear modulus value measured by rheometry for the carbon-carbon specimens was 5.8 GPa (0.84 Msi), which closely corresponds to values

obtained by mechanical testing, 5.5 GPa (0.8 Msi), and values reported in the literature, 5 GPa (0.73 Msi)[7].

An exponentially decaying shear modulus trend is observed in Figure 11 for measurements of seventeen different specimens obtained at varied oxidation time intervals.

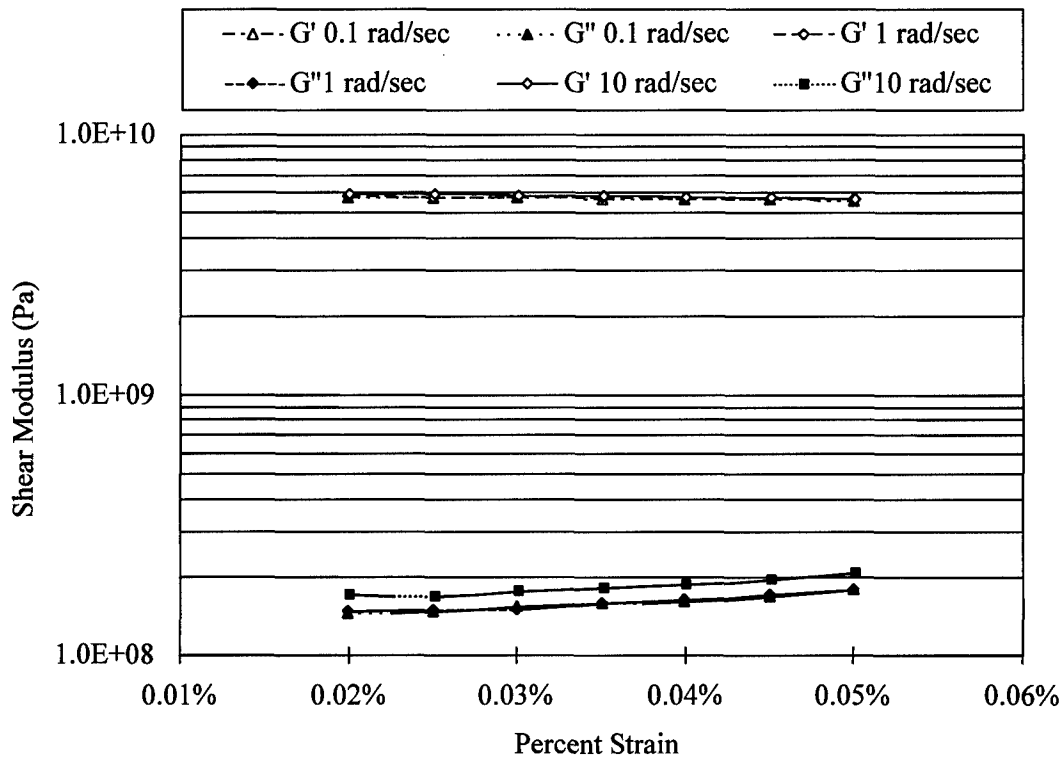


Figure 10. Shear Modulus Measurement of a Typical Unoxidized Carbon-Carbon Specimen

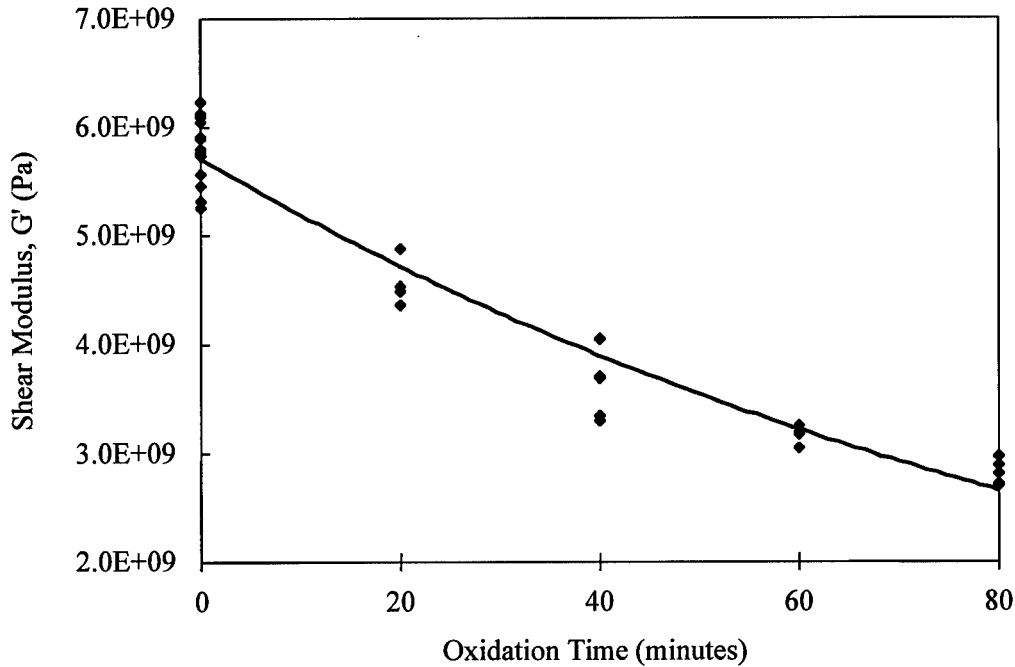


Figure 11. Shear Modulus Degradation Due to Oxidation at 900 °C

iii. Electrical Resistance

The change in electrical resistance of a typical specimen exposed for eighty minutes is presented in Figure 12. An increase in the slope of the electrical resistance is revealed between fifteen and twenty minutes after exposing the carbon-carbon to compressed air at 900°C. Subtracting the initial electrical resistance value of each specimen from its electrical resistance data recorded eliminated the variations in the initial electrical resistance values of the samples and determined the representative electrical resistance for each specimen, allowing a comparison between specimens. A summary of the representative electrical resistance with increasing oxidation time for the seventeen individual specimens oxidized at 900°C for periods of twenty, forty, sixty, or eighty minutes is displayed in Figure 13. A trend similar to that of the typical specimen shown in Figure 12 is observed. The increased electrical resistance slope after twenty minutes indicates the preferential oxidation of the carbon fibers as compared to the oxidation of the matrix.

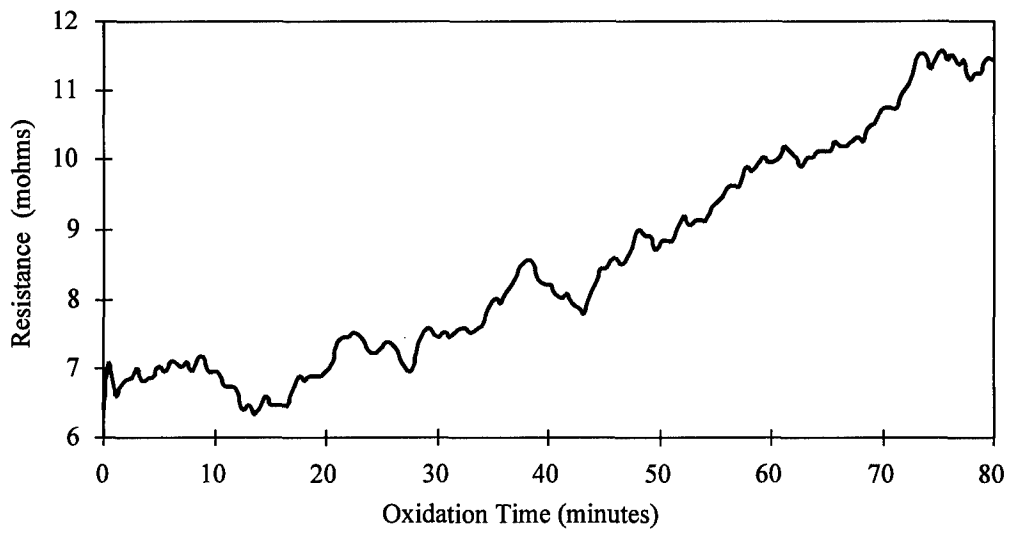


Figure 12. *Electrical Resistance versus Oxidation for a Typical C-C Specimen*

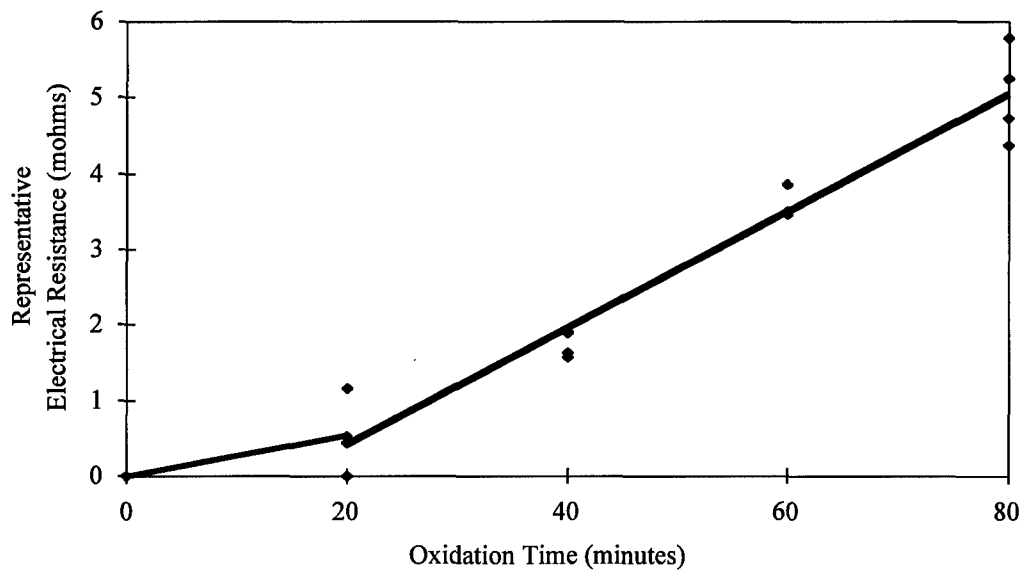


Figure 13. *Representative Electrical Resistance versus Oxidation Time for Seventeen Individual C-C Specimens*

V. Analysis

i. Microscopy

The specimens after different lengths of exposure time were carefully examined with SEM. The regions of interest were the SiC coating, the carbon fiber bundles, and the carbon matrix.

The thermal mismatch, due to large differences in CTE between SiC and the carbon-carbon substrate, produced cracks in the coating, see Figure 14. After forty minutes of exposure at 900 °C, additional new cracks developed and penetrated further into the substrate. After eighty minutes, the crack density increased and clearly moved into the carbon matrix, but, the coating and the carbon-carbon interface seemed to remain intact.

Fiber tows, both longitudinal and transverse to the cross section viewed, revealed preferential oxidation after forty minutes as shown in Figure 15. The physical disappearance of the transverse fibers occurred first and was quite visible, see Figure 16. After sixty minutes of exposure, the loss in the longitudinal fibers was increasingly evident as well.

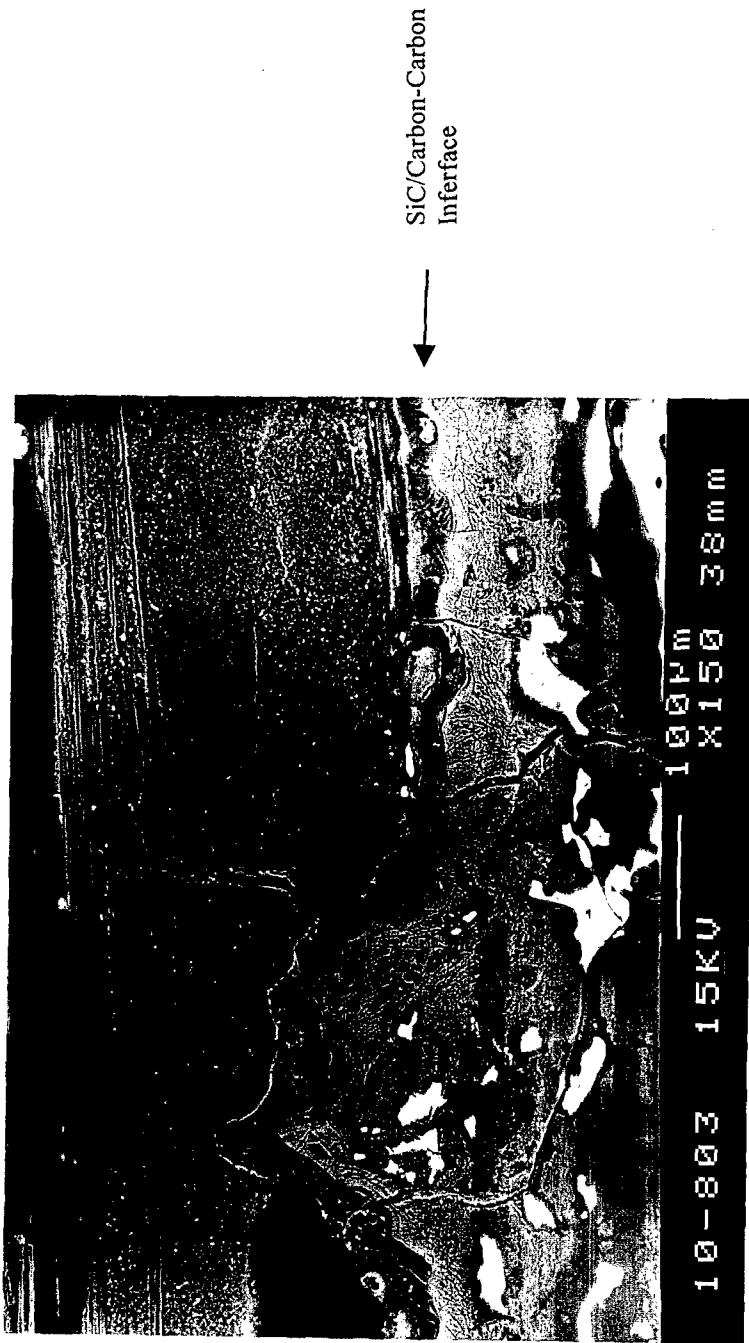


Figure 14. Cracks in SiC

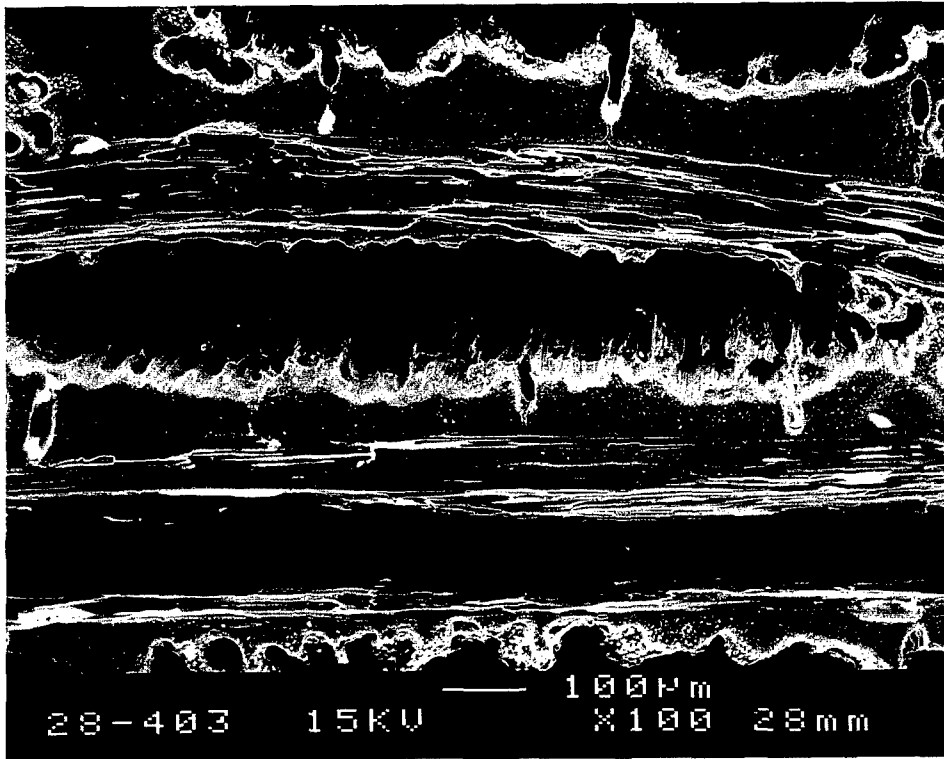


Figure 15. Preferential Fiber Bundle Oxidation after Forty Minutes

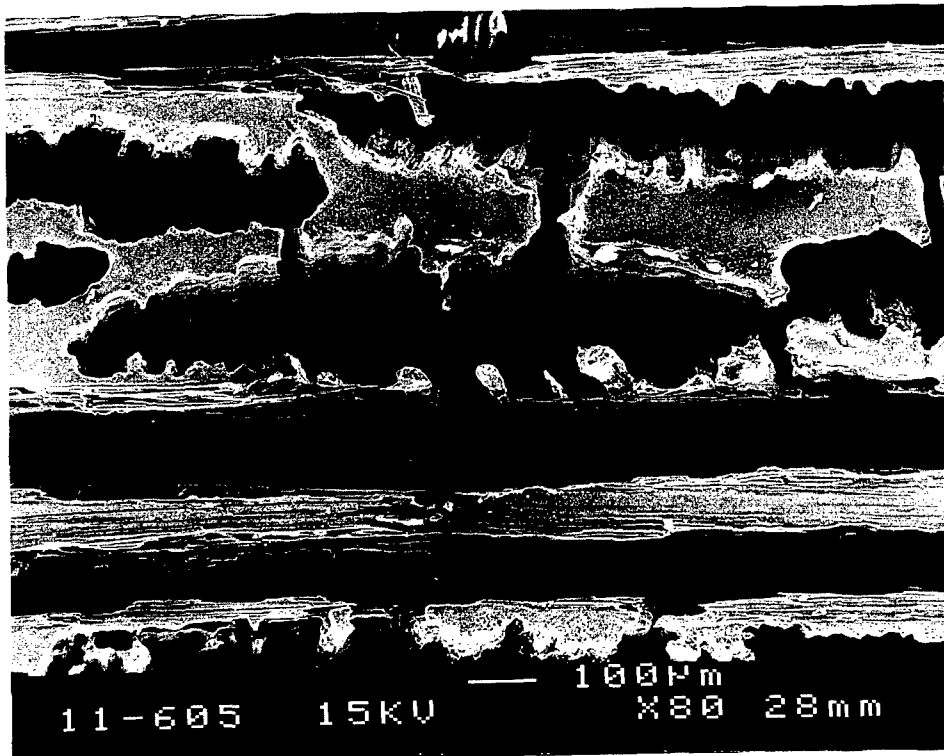


Figure 16. Transverse Fiber Bundle Damage

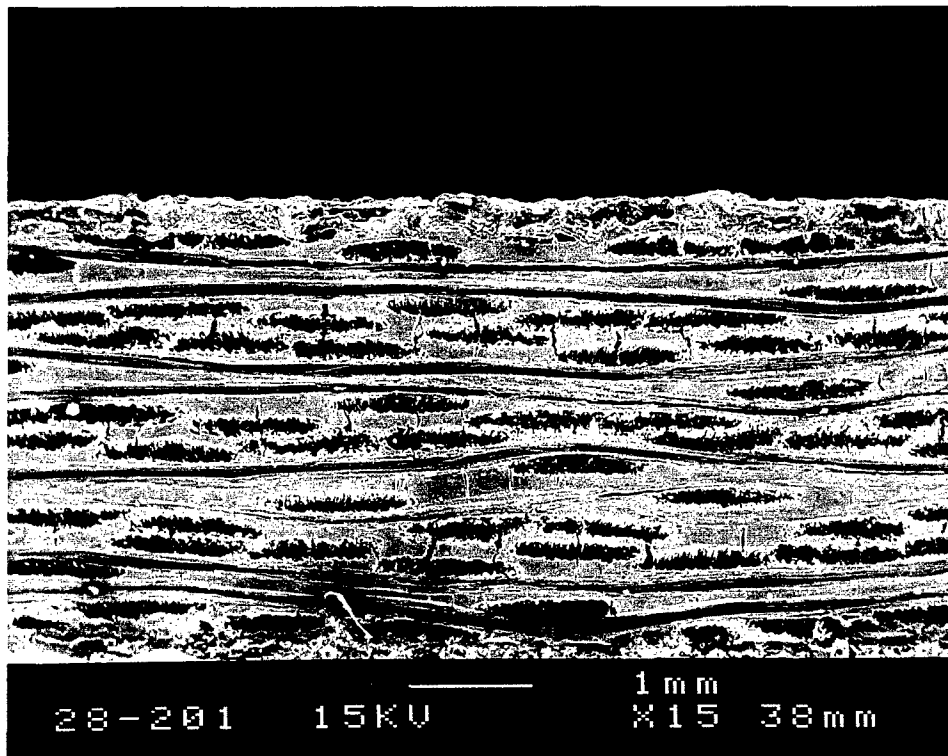


Figure 17. Initial Matrix Cracking after Twenty Minutes of Oxidation

Within the first twenty-minute oxidation period, matrix damage of the carbon-carbon was limited to line cracks, shown in Figure 17 and Figure 18. After forty minutes of exposure, the density and the physical dimensions of the cracks increased in width and length. The cracks seemed to be confined to the matrix and did not bridge the fibers. The matrix was greatly diminished after sixty minutes but no new crack initiation sites seemed to develop as shown in Figure 19.

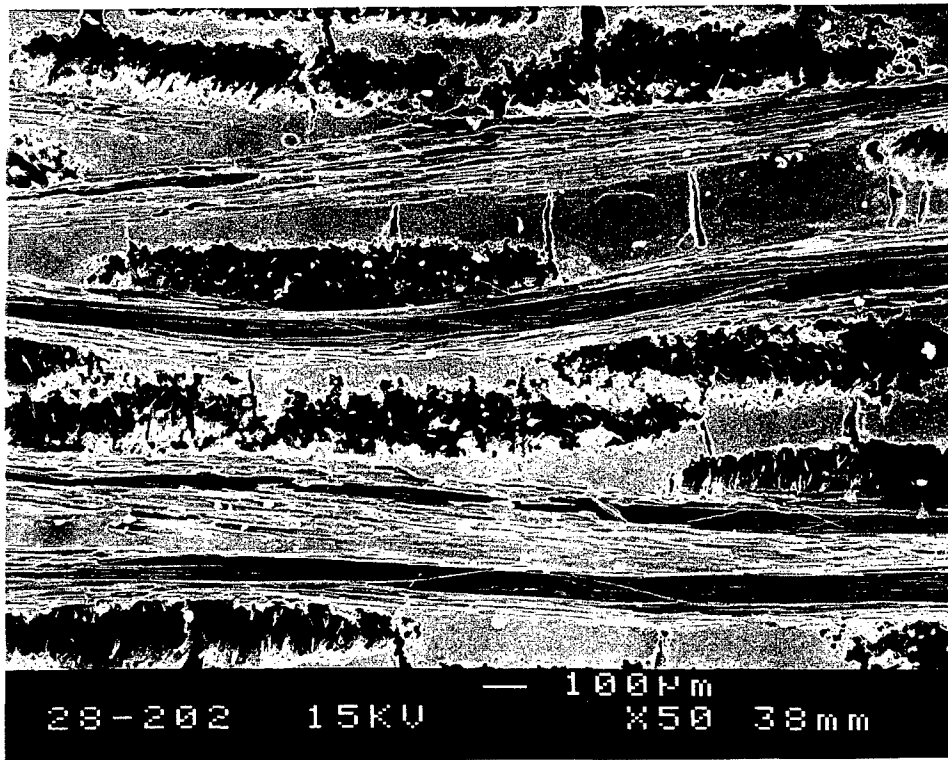


Figure 18. Initial Crack Growth after Twenty Minutes

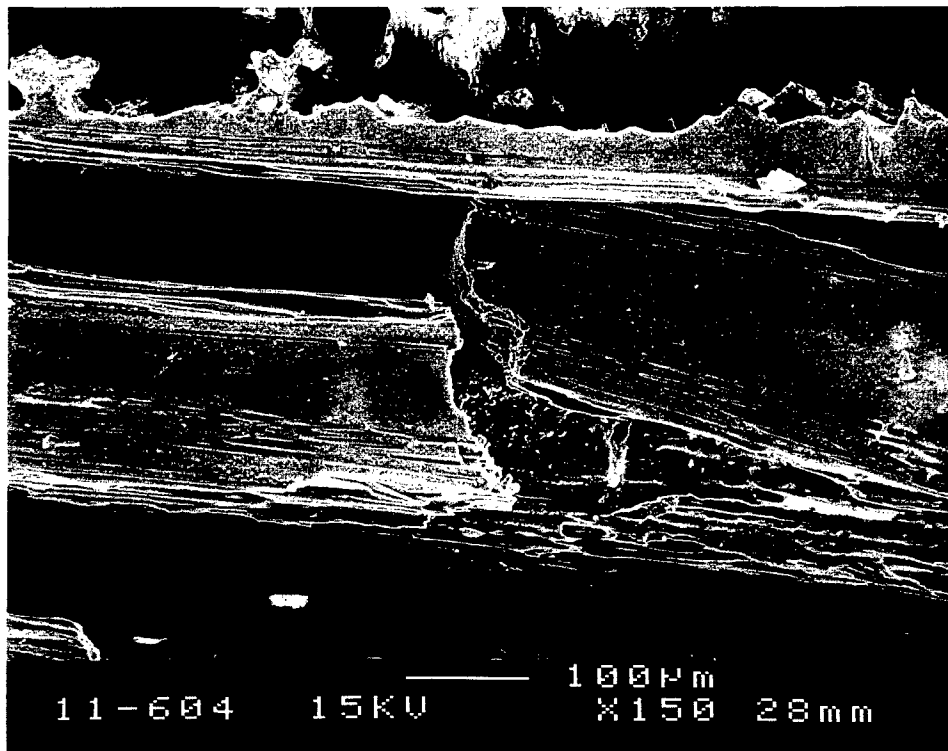


Figure 19. Matrix Degradation after Sixty Minutes of Oxidation

ii. Diffusion

Oxidation of carbon-carbon above 700 °C is limited by the diffusion of oxygen into the carbon surface and proceeds according to the following chemical reaction [1,3]



The oxidation loss is proportional to time and may be represented as

$$W = \frac{(C_g - C_r)}{\delta} D_f t \quad (15)$$

Where W is the oxidation loss, C_g is the concentration of reactant gas in the gas stream, C_r is the concentration of the reactant gas at the exterior surface of the reacting specimen, D_f is the diffusion coefficient of the reactant through the boundary layer, and t is time. The parameters C_g , C_r , D_f , and δ are not functions of the surface area [3]. Consequently, even though the surface area of the carbon-carbon susceptible to oxidation increases with time the oxidation rate remains constant for a steady state temperature [1].

iii. Mass Loss

The constant mass loss indicates that the oxidation is controlled by the diffusion of oxygen into the carbon-carbon. This agrees with both the diffusion equation presented in the literature [1] and experimental data reported [1,3,12] for diffusion controlled oxidation of carbon-carbon. Initially cracks develop in the matrix and preferential oxidation of the fibers occurs. Fiber bundles both transverse and longitudinal are greatly diminished and the crack density within the matrix increases with increased oxidation time. The development of cracks increases the surface area susceptible to oxidation, but the rate of oxidation remains constant; consequently, the crack growth rate is slowed.

iv. Resistance

a. Analytical Time Simulation

1. Assumptions

The coating SiC is unaffected by the oxidation conditions and consequently there is no volume change in SiC. The resistivity of SiC will change with temperature but is

assumed to remain constant at 900°C. Therefore, for simplicity, the coating contributions will be neglected.

The electrical resistivity of the carbon matrix is assumed to be proportional to the electrical resistivity of the carbon fibers. It is also assumed that the electrical resistivity of the matrix is greater than the electrical resistivity of the fiber because of the incipient heterogeneities in the matrix. Consequently, the proportionality constant, β , is greater than one.

2. Bulk Resistance

Microscopy micrographs of specimens exposed for forty minutes revealed both longitudinal and transverse fiber losses, which cause the reduction in the fiber volume fraction. This suggests that with increased oxidation time the electrical resistance of the carbon-carbon specimen becomes increasingly controlled by the electrical resistivity of the matrix.

The electrical resistance of the carbon-carbon specimen (CC substrate, SiC coating and the borate glass) at 900°C is expressed as

$$R_{\text{Bulk}} = \frac{L^2}{\frac{V_{\text{SiC}}}{\rho_{\text{SiC}}} + \frac{V_m}{\rho_m} + \frac{V_f}{\rho_f} + \frac{V_{\text{B}_2\text{O}_3}}{\rho_{\text{B}_2\text{O}_3}}} \quad (17)$$

Neglecting SiC coating the expression for resistance becomes

$$R_{\text{Bulk}} = \frac{L^2}{\frac{V_m}{\rho_m} + \frac{V_f}{\rho_f} + \frac{V_{\text{B}_2\text{O}_3}}{\rho_{\text{B}_2\text{O}_3}}} \quad (17a)$$

Where ρ_f is the electrical resistivity of the fibers, ρ_m is the electrical resistivity of the matrix, V_f is the volume of the fibers, and V_m is the volume of the matrix. Eq(17a) can then be rewritten as eq(17b).

$$R_{\text{Bulk}} = \frac{\rho_f \rho_m \rho_{\text{B}_2\text{O}_3} L^2}{V_m \rho_f \rho_{\text{B}_2\text{O}_3} + V_f \rho_m \rho_{\text{B}_2\text{O}_3} + V_{\text{B}_2\text{O}_3} \rho_f \rho_m} \quad (17b)$$

V_f , V_m , and $V_{\text{B}_2\text{O}_3}$ can then be written in terms of a fiber volume fraction, f_v , a boric oxide volume fraction, B_v , and the total volume, V .

$$V_f = V f_v \quad (18)$$

$$V_{\text{B}_2\text{O}_3} = V B_v \quad (19)$$

$$V_m = V(1 - f_v - B_v) \quad (20)$$

Based on the assumption of proportionality, ρ_m is given as

$$\rho_m = \beta \rho_f \quad (21)$$

Substituting equations (18), (19), (20), and (21) into eq(17a) gives eq(22).

$$R_{\text{Bulk}} = \frac{L^2 \rho_f \rho_b \beta}{V[\beta \rho_{\text{B}_2\text{O}_3} f_v + \beta \rho_f B_v + \rho_{\text{B}_2\text{O}_3} (1 - f_v - B_v)]} \quad (22)$$

Eq(22) can be simplified to the basic resistance equation of

$$R_{\text{Bulk}} = \frac{\rho_{\text{Bulk}} L_r}{A_r} \quad (23)$$

Where the bulk resistivity, ρ_{Bulk} , is

$$\rho_{\text{Bulk}} = \frac{\rho_f \rho_b \beta}{\beta \rho_{\text{B}_2\text{O}_3} f_v + \beta \rho_f B_v + \rho_{\text{B}_2\text{O}_3} (1 - f_v - B_v)} \quad (24)$$

Eq(22) in conjunction with SEM observations and knowledge of inhibitor characteristics can be used to describe the change in electrical resistance trend displayed in the data.

Observations from the SEM micrographs indicated that within the first twenty minutes of oxidation, some fiber loss occurs and matrix cracking initiates. Therefore, the initial fiber volume fraction, 60% [13], is assumed to remain constant for the first twenty minutes of oxidation while reduction in total volume takes place. SEM studies also revealed increased preferential oxidation of the carbon fibers after twenty minutes of oxidation. Consequently, it was assumed that as oxidation time increases both the fiber volume fraction and the total volume decrease.

The carbon-carbon specimen contains boron carbide, B_4C , which converts to boric oxide, B_2O_3 [14,15]. B_2O_3 is a viscous glass that inhibits oxygen infiltration by filling the cracks and voids in the specimen. It volatilizes at temperatures near $800^\circ C$ [7]. Consequently, the inhibitor volume fraction decreases with respect to oxidation time. It is initially assumed that the inhibitor volume fraction of the specimen is about 12% of the total volume of the carbon-carbon matrix, about 5% of the total volume, [13] and decreases with time.

The analytical trends of the normalized electrical resistance as a function of oxidation time as determined by eq(17b) for various proportionality constants and varied inhibitor volume fractions are displayed in Figure 20 and Figure 21. The proportionality constants range from 5 to 1000. The total volume reductions used to generate Figure 20 and Figure 21 were taken from experimental measurements of the carbon-carbon specimens. The total volume reduction, fiber volume fractions, and inhibitor volume fractions used to generate Figure 20 and Figure 21 are shown in Table 2. In order to determine the sensitivity of the analytical model to the inhibitor volume fraction, two cases were considered; namely the inhibitor volume fraction was reduced linearly (Figure 20) and it was treated to remain constant at 4.8% (Figure 21). A comparison of Figure 20-21 shows that the normalized resistance in Figure 20 is slightly greater than the normalized resistance in Figure 21. However, the differences generated by the inhibitor volume fraction are negligible in comparison to the contributions from the carbon fibers and the carbon matrix.

Table 2. Analytical Simulation Parameters for Inhibitor Volume Fraction Reduction

Oxidation Time Minutes	Total Volume Percentage V	Fiber Volume Fraction f_v	Boron Volume Fraction B_v , constant	Boron Volume Fraction B_v variable
0	100%	60%	4.8%	4.8%
20	94%	60%	4.8%	3.6%
40	91%	52%	4.8%	2.4%
60	83%	49%	4.8%	1.2%
80	80%	45%	4.8%	0.0%

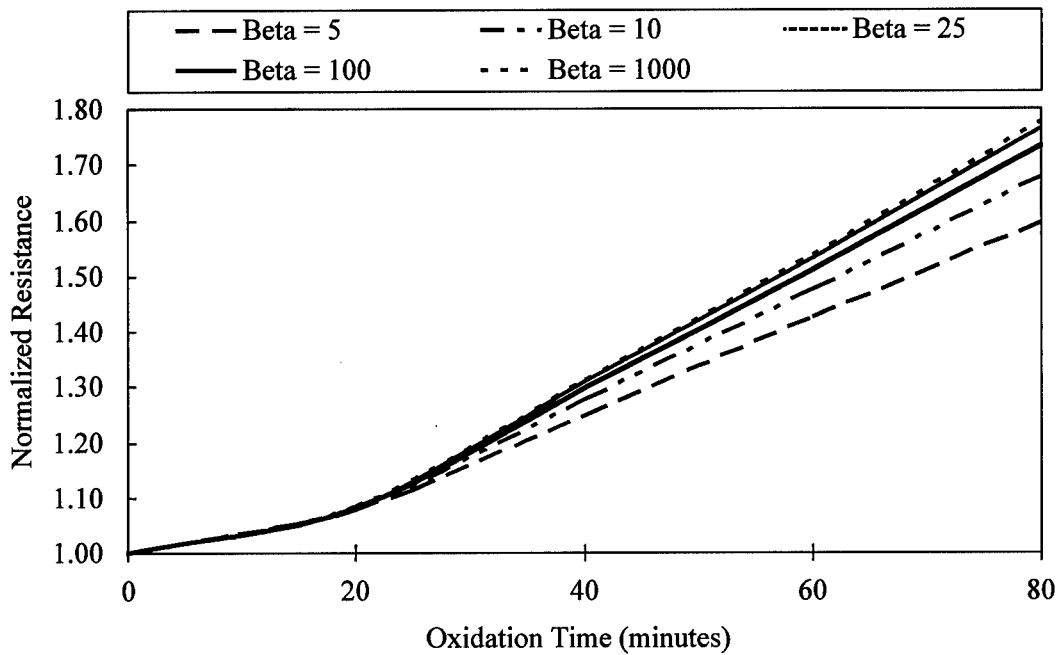


Figure 20. Analytical Simulation with Inhibitor Volume Fraction Reduction

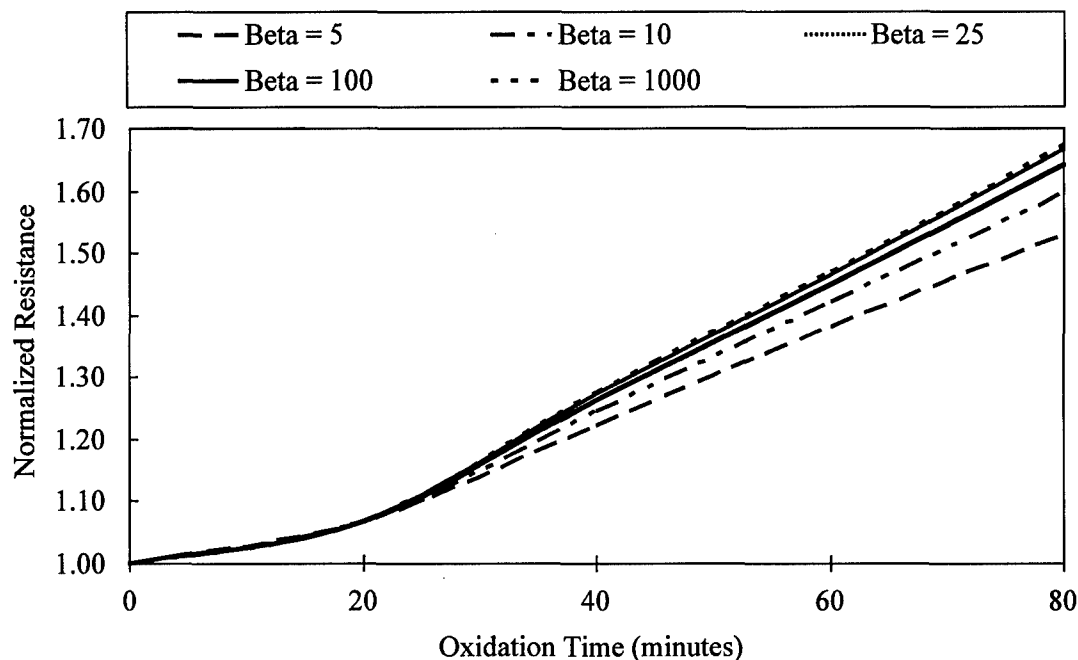


Figure 21. Analytical Simulation with Constant Inhibitor Volume Fraction

The slope of the electrical resistance increases after twenty minutes of oxidation. This is attributed to the time period when the fiber bundles start to preferentially oxidize which implies that the current is now primarily passing through the carbon matrix, a path with increased resistivity. One can also conclude that although the surface area susceptible to oxidation is increasing, the rate of oxidation is not, which agrees with reports in the literature [10] and the mass loss results.

b. Analytical Mass Simulation

The bulk resistance of the carbon-carbon specimen can be written in the general form as

$$R_{\text{Bulk}} = \frac{\rho_{\text{Bulk}} L_r}{A_r} \quad (25)$$

A_r is the cross sectional area of the specimen perpendicular to the input current, L_r is the length between potential measuring contacts, and ρ_{Bulk} is the bulk resistivity of the specimen. A_r is approximated as

$$A_r = \frac{V}{L_s} \quad (26)$$

where V is volume, and L_s , the total length of the specimen. Subsequently, V can be expressed in terms of the mass of the specimen, m , and the density, γ .

$$V = \frac{m}{\gamma} \quad (27)$$

Since mass changes as a function of oxidation, its effect on volume change is illustrated with percent mass loss, $\% \Delta m$, and the initial volume of the sample, V_{0s} .

$$V = \frac{V_{0s}(100 - \% \Delta m)}{100} \quad (28)$$

Substitution of equations (26), (27), and (28) into eq(25) provides the bulk resistance, R_{Bulk} , in terms of L_s , L_r , ρ_{Bulk} , V_{0s} , and $\% \Delta m$.

$$R_{Bulk} = \frac{100 \rho_{Bulk} L_r L_s}{V_{0s}(100 - \% \Delta m)} \quad (29)$$

Oxidation degrades the carbon-carbon specimen as a whole and is better described in terms of the specimen volume, as opposed to the cross sectional area and length. Therefore, it is assumed that the affect of oxidation on the specimen length, L_s , is taken into account by the volume fraction terms in ρ_{Bulk} . Consequently, L_s is assumed to remain constant. The time dependent terms in eq(29) are ρ_{Bulk} and $\% \Delta m$. The percent mass loss, $\% \Delta m$, was experimentally determined to linearly increase, leading to an increase in the electrical resistance of the specimen. The bulk resistivity, ρ_{Bulk} , also increases with oxidation time since it is strongly dependent on the fiber volume fraction, f_v , and the boric oxide volume

fraction, B_v . ρ_{Bulk} was previously derived as eq(24). Inclusion of the SiC coating in the resistivity yields

$$\rho_{Bulk} = \frac{\beta \rho_f \rho_{B_2O_3} \rho_{SiC}}{S_v \beta \rho_f \rho_{B_2O_3} + f_v \beta \rho_{SiC} \rho_{B_2O_3} + B_v \beta \rho_f \rho_{SiC} + \rho_{SiC} \rho_{B_2O_3} (1 - f_v - B_v - S_v)} \quad (30)$$

where S_v is the SiC volume fraction percentage and V_m is now

$$V_m = V(1 - f_v - B_v - S_v) \quad (31)$$

Eq (30) can be arranged as

$$\rho_{Bulk} = \frac{\beta \rho_f}{\frac{S_v \beta \rho_f}{\rho_{SiC}} + \frac{B_v \beta \rho_f}{\rho_{B_2O_3}} + 1 + f_v (\beta - 1) - B_v - S_v} \quad (32)$$

Eq(32) clearly shows that ρ_{Bulk} is inversely proportional to f_v . More importantly, it can be seen that for large values of ρ_{SiC} and $\rho_{B_2O_3}$ relative to $\beta \rho_f$, the first two terms in the denominator are small in comparison to the others. Resistivity values for the respective constituents at 900°C are presented in Table 3 [16, 17].

Table 3. Resistivity Values of C-C Constituents at 900 °C

Material	Electrical Resistivity $\Omega \cdot m$
SiC	200
B_2O_3	100
Carbon Fiber	5×10^{-6}

Note the SiC used in this application is assumed to have a high electrical resistivity because of the development of cracks in the SiC coating during manufacturing due to the mismatch in

the CTE with the carbon-carbon substrate and other heterogeneities introduced during CVD application. Simplification of eq(32) based on the values in Table 3 yields

$$\rho_{\text{Bulk}} = \frac{\beta \rho_f}{1 + f_v (\beta - 1) - B_v - S_v} \quad (33)$$

Consequently, ρ_{Bulk} is controlled primarily by ρ_f , β , and the respective volume fractions of the constituents. Furthermore, it can be seen that for large values of β , ρ_{Bulk} becomes

$$\rho_{\text{Bulk}} = \frac{\rho_f}{f_v} \quad (34)$$

The increase in the electrical resistance as a function of the percent mass loss for specimens oxidized at 900°C for twenty, forty, sixty, or eighty minutes can be clearly observed in Figure 22. The analytical approximation, eq(29), follows the data realistically. Based on the relative magnitudes of the resistivities of SiC and B₂O₃ as compared to the resistivity of the carbon fibers, ρ_{Bulk} was determined from eq(33). The value of β was assumed to be 100 as a result of the parametric studies conducted with the analytical time simulation. The values used for the respective volume fractions and percent mass loss are shown in Table 4. The average initial experimental electrical resistance, R_{0I} , of seventeen specimens is 8 mΩ. The average initial experimental bulk resistivity, ρ_{BulkI} , is obtained as $13 \times 10^{-6} \Omega \cdot \text{m}$. Substituting ρ_{BulkI} , into eq(33) provided an initial average experimental value for fiber resistivity, ρ_{fI} , as $6.69 \times 10^{-6} \Omega \cdot \text{m}$, which was used in eq(33) in conjunction with eq(29) to determine the analytical curve. The value of ρ_{fI} , $6.69 \times 10^{-6} \Omega \cdot \text{m}$, is within 33% of the reported literature value, $5 \times 10^{-6} \Omega \cdot \text{m}$.

Table 4. Analytical Simulation Parameters for eq(29) and eq(33)

Percent Mass Loss % Δm	Volume Fraction		
	Fiber f_v	B ₂ O ₃ B _v	SiC S _v
0.0%	51.32%	4.10%	28.95%
5.1%	51.32%	3.08%	30.50%
10.2%	44.48%	2.05%	32.24%
15.3%	41.91%	1.03%	34.18%
20.4%	38.49%	0.00%	36.37%

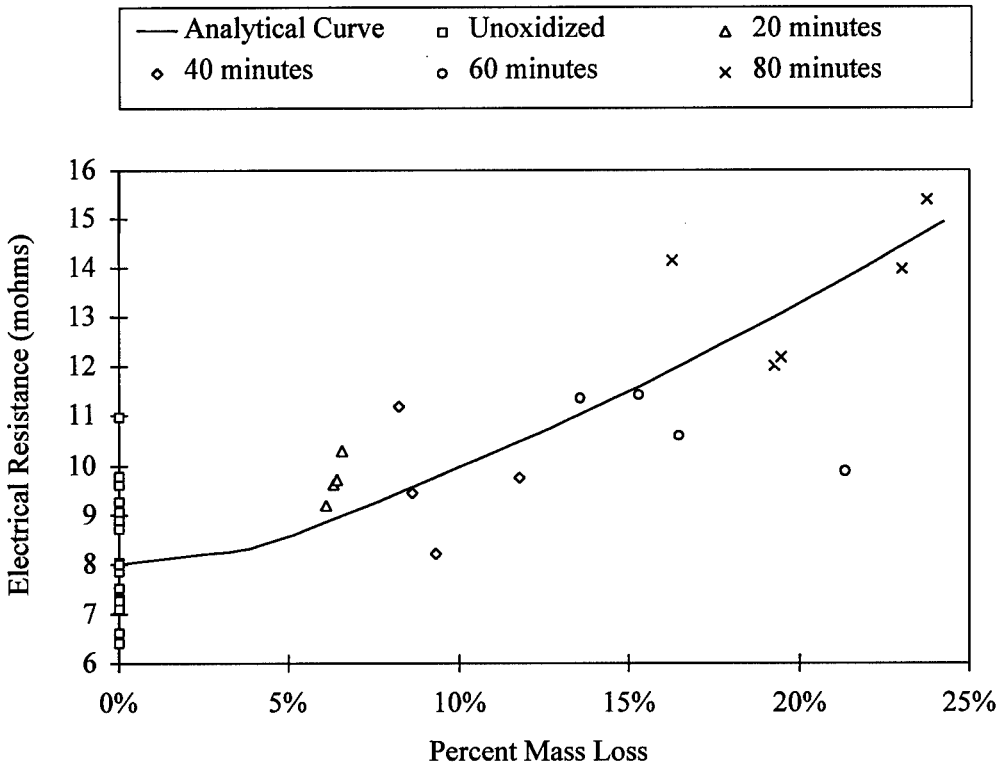


Figure 22. Electrical Resistance versus Percent Mass Loss for Seventeen Specimens

The initial resistance value of each specimen is subtracted from its respective measured value to reduce scatter in the data and to provide a representative electrical resistance for each specimen. The representative electrical resistance for specimens oxidized at 900°C as a function of the percent mass loss along with the analytical prediction are shown in Figure 23. Note that the predictions follow the representative electrical resistance data realistically.

The relationship between the experimental results and the analytical curves in Figure 22 and Figure 23 seem to confirm the strong dependence of the electrical resistance on the fiber volume fraction, f_v , the fiber resistivity, ρ_f , and the matrix resistivity, $\beta\rho_{ff}$. This is in agreement with results from the analytical time simulation.

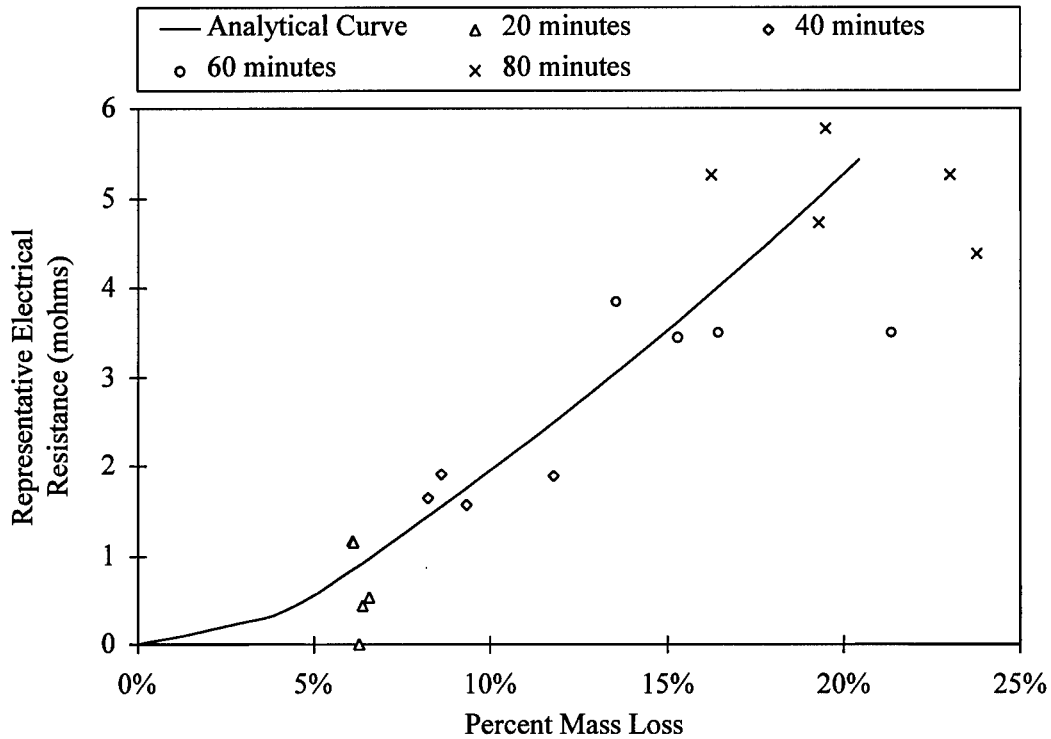


Figure 23. Representative Electrical Resistance for Seventeen Specimens versus Percent Mass Loss

v. Shear Modulus

The shear modulus is a matrix dominated property; therefore, shear modulus degradation corresponds primarily to increased matrix damage. Shear modulus degradation within the first forty minutes is related to the increase in crack length, crack widths, and crack density experienced within the matrix. After the initial forty-minute crack growth period, the rate of shear modulus degradation is decreased. As oxidation time increases the surface areas susceptible to the diffusion reaction is increased, however, the rate of oxidation remains constant. Physically, this corresponds to a reduction in crack growth rate, crack density saturation, within the matrix and the reduction of the shear modulus degradation rate.

A comparison of the shear modulus to the percent mass loss is shown in Figure 24. Note that the trend is the same as the trend seen for the comparison of the shear modulus to time.

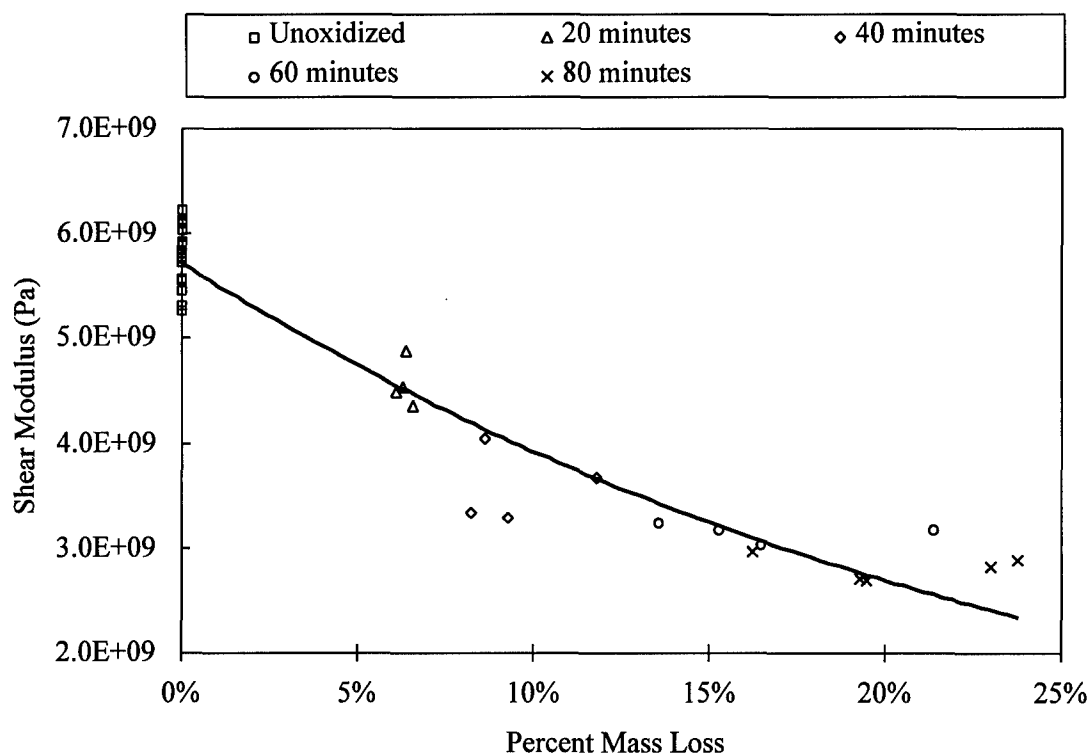


Figure 24. Shear Modulus as Compared to Percent Mass Loss at 900 °C

The empirical relationship between the shear modulus and the electrical resistance for carbon-carbon oxidized at 900°C is shown in Figure 25. Seventeen specimens oxidize at twenty, forty, sixty, or eighty minutes were used to determine the exponentially decreasing relationship as illustrated by the solid line fit in Figure 25. The dashed lines indicate one standard deviation above and below the trend, ± 0.5 GPa. Note that with the exception of two sixty-minute specimens and one forty minute specimen most of the oxidized specimens fall near or within one standard deviation.

As a comparison to the experimental data in Figure 25 the analytical electrical resistance simulations has been added to the experimental shear modulus data in Figure 24 to produce Figure 26. For a given mass loss both the shear modulus and the analytical electrical resistance can be determined from Figure 26. Note that, the shear modulus determined from Figure 26 can then be used to determine an experimental electrical resistance value using

Figure 25. As an example for the 5% mass loss the experimental shear modulus is approximately 4.8 GPa and the analytical electrical resistance is 8.55 mohms as determined from Figure 26. From Figure 25 it can be seen that for a shear modulus of 4.8 GPa the experimental electrical resistance value is approximately 9.0 mohms, which is a 5% difference. Additional comparisons of the experimental electrical resistance to the analytical resistance were done for percent mass loss values of 0%, 10%, 15%, and 20% and the results are shown in Table 5.

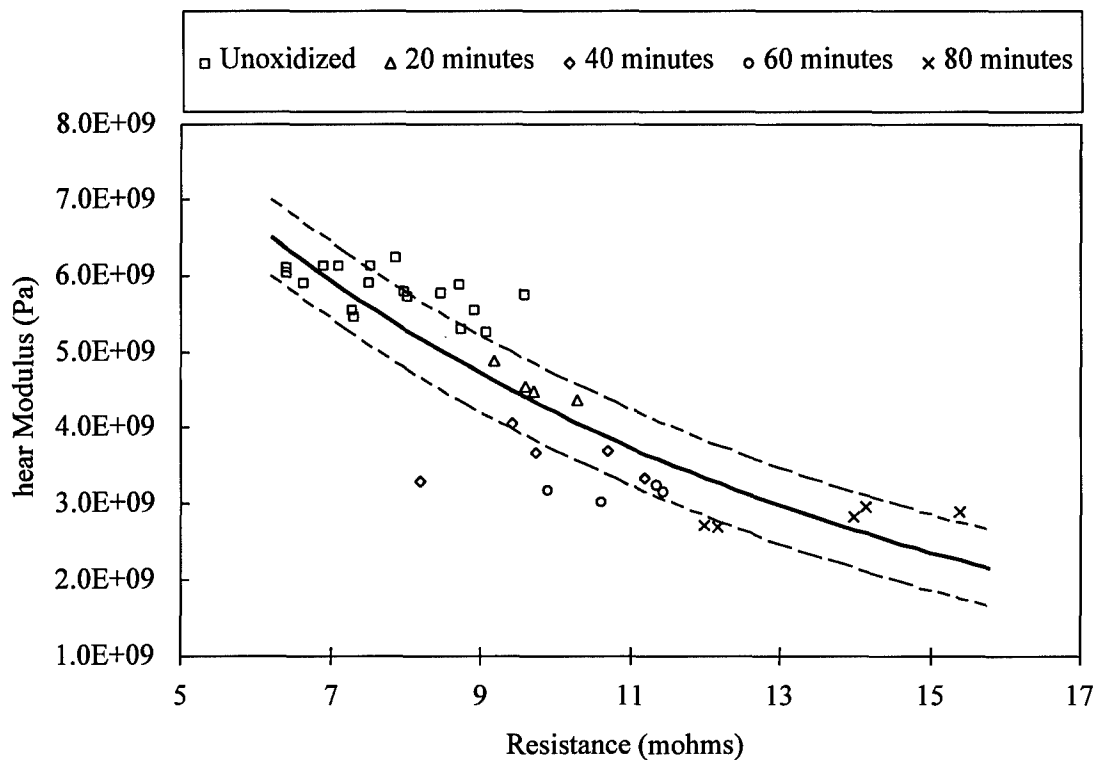


Figure 25. Shear Modulus versus Electrical Resistance for Carbon-Carbon at 900°C

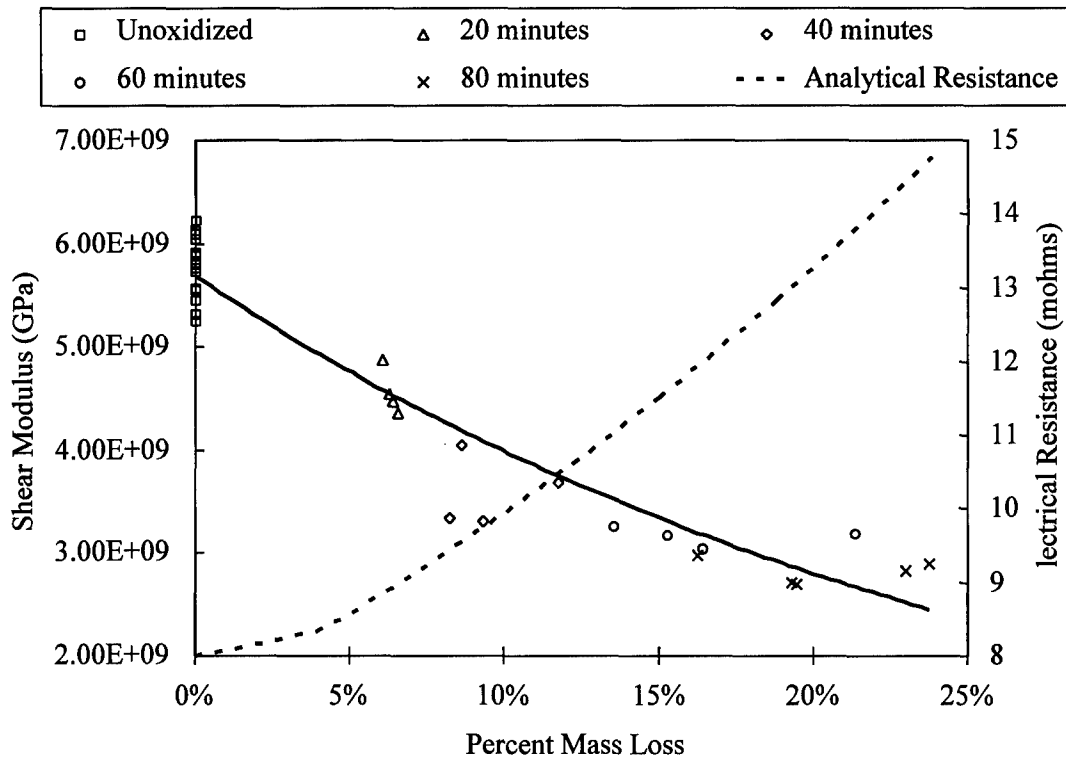


Figure 26. Experimental Shear Modulus and Analytical Electrical Resistance as Compared to Percent Mass Loss

Table 5. Shear Modulus and Electrical Resistance Correlation with Mass Loss

Percent Mass Loss $\Delta m\%$	Experimental Shear Modulus GPa	Experimental Electrical Resistance mohms	Analytical Electrical Resistance mohms	Percent Difference
0	5.8	7.25	8.00	10.3
5	4.8	9.00	8.55	5.0
10	4.0	10.40	9.95	4.3
15	3.4	11.75	11.51	2.0
20	2.8	13.50	13.27	1.7

The results show that the analytical simulation is on average within 4.7% of the averaged experimental value. Also correlation between the percent mass loss and both the shear modulus and the electrical resistance are illustrated from Table 1 results.

Consequently, for a given value of either the shear modulus, electrical resistance, or mass loss the other two values can be determined.

VI. Conclusions

Oxidation of the carbon-carbon at 900°C, is observed to be diffusion controlled. Initial oxidation damage of the specimen was due primarily to the loss of transverse and longitudinal fiber bundles. Fiber bundle losses encourage increased matrix degradation which lead to crack initiation and growth. For oxidation times in excess of sixty minutes, A reduction in the crack growth rate develops because the surface area susceptible to oxidation increases yet the oxidation rate remains constant.

Electrical resistance of the carbon-carbon specimen increased exponentially with increased oxidation time and mass loss. The electrical resistance change due to oxidation of the carbon-carbon substrate is controlled primarily by the bulk electrical resistivity, which is a matrix controlled property. As oxidation increases the electrical properties of the carbon-carbon specimen approach the electrical properties of the carbon matrix. Bulk electrical resistivity dependence on the matrix volume fractions showed an abrupt increase in slope within the first forty minutes of oxidation indicating the oxidation mechanism changed from preferential fiber bundle damage to increased matrix damage.

Shear modulus degradation decreased exponentially with increased oxidation time and mass loss. The exponentially decreasing trends indicate the reduction in both crack initiation and crack growth rate with increased oxidation time.

The analytical electrical resistance model is able to determine shear modulus values of the carbon-carbon specimens for the experimental conditions given, typically within 5%. A relationship exist between the percent mass loss, shear modulus, and the electrical resistance, which allows one type of measurement, mass loss, shear modulus, or electrical resistance, to determine the other two values. Consequently, electrical resistance measurements could be used to determine both the percent mass loss and the shear modulus value for a given specimen.

The deviations in the electrical resistance readings were believed to be caused primarily by the incipient heterogeneities within each respective specimen. Some errors in determining the electrical resistance may have also been introduced at the electrical contact points of some specimens.

i. Recommendations

The electrical resistivity of this carbon-carbon is about $13 \times 10^6 \Omega \cdot m$. Consequently, the electrical resistance measurements at $900^\circ C$ were in the milli-ohm range. Increasing the size of the specimen would reduce errors in reading the electrical resistance.

VII References

1. Savage, G. 1993. *Carbon-Carbon Composites*. London: Chapman & Hall.
2. Kalapakjian, Serope 1992. *Manufacturing Engineering and Technology Second Edition*. New York: Addison-Wesley Publishing Company.
3. Thomas, C.R. 1993. *Essentials of Carbon-Carbon Composites*. Cambridge: The Royal Society of Chemistry.
4. Wu, Tsung-Ming, Wen-Cheng Wei and Shu-en Hsu. 1991. "On the Oxidation Kinetics and Mechanisms of Various SiC-Coated Carbon-Carbon Composites," *Carbon*, 29(8): 1257-1265.
5. Hatta, Hiroshi, Yasuo Kogo, Toshio Yarii, Yoshinodai, Sagamihara, Higashi-machi and Tajimi. 1996. "Oxidation Behavior of Carbon/Carbon Composites in Re-entry Environment," *AIAA-96-1374*:1-10.
6. Runyan, W.R. 1975. *Semiconductor Measurements and Instrumentation*. New York: McGraw Hill Book Company.
7. Elliott, Charles H. and Ozden O. Ochoa. 1995. "Oxidation for C-C Composites: Inhibitor/Substrate Interaction," *The Tenth International Conference on Composite Materials*. Paper 352.
8. Rheometrics Owner's Manual 1990. *Rheometrics Mechanical Spectrometer/Dynamic Spectrometer RMS-800/RDSII*. New Jersey: Rheometrics Incorporated.
9. McCrum, N. G., C.P. Buckley and C.B. Bucknall 1988. *Principles of Polymer Engineering*. New York: Oxford University Press Incorporated.
10. Rheometrics Owner's Manual 1990. *Rheometrics Mechanical Spectrometer/Dynamic Spectrometer RMS-800/RDSII*. New Jersey: Rheometrics Incorporated.
11. Keithley Instruments 1990. *Model 237 High Voltage Source Measure Unit Operator's Manual*. Ohio: Keithley Instruments.
12. McKee, D.W. 1987. "Oxidation Behavior and Protection of Carbon/Carbon Composites," *Carbon*, Vol 25. No. 4 :551-557.
12. Ahsley, Tim Harold 1996. *Structural Response of Oxidation Resistant Carbon-Carbon Composites*. Masters Thesis, Department of Mechanical Engineering, Texas A&M University

14. Sheehan, James E. 1989. "Oxidation Protection for Carbon Fiber Composites," *Carbon*, Vol. 27 No. 5 :709-715.
15. Matkovich, V. I. 1977. *Boron and Refractory Borides*. New York: Springer-Verlag.
16. Touloukian, Y.S. 1967. *Thermophysical Properties of High Temperature Solid Materials Volume 5*. New York: The MacMillan Company.
17. Scholze, Horst 1991. *Glass Nature, Structure, and Properties*. New York: Springer-Verlag New York, Incorporated.